Journal of Physiology (1993), **472**, *pp.* 203–231
With 13 figures
Printed in Great Britain

CHANGES IN SODIUM AND CALCIUM CHANNEL ACTIVITY FOLLOWING AXOTOMY OF B-CELLS IN BULLFROG SYMPATHETIC GANGLION

BY BALVINDER S. JASSAR, PETER S. PENNEFATHER* AND PETER A. SMITH

From the Department of Pharmacology, University of Alberta, Edmonton, Alberta, Canada, T6G 2H7

(*Received 24 November 1992*)

SUMMARY

1. Currents mediated by Ca^{2+} channels using Ba^{2+} as a charge carrier (I_{Ba}), Na^+ currents (I_{Na}) and voltage- and Ca^{2+}-dependent K^+ currents (I_C) were recorded from bullfrog paravertebral sympathetic ganglion B-cells using whole-cell patch-clamp recording techniques. Currents recorded from control cells were compared with those from axotomized cells 13–15 days after transection of the postganglionic nerve.

2. Axotomy reduced peak I_{Ba} at -10 mV (holding potential $= -80$ mV) from $3{\cdot}3 \pm 0{\cdot}3$ nA ($n = 42$) to $1{\cdot}7 \pm 0{\cdot}1$ nA ($n = 39$, $P < 0{\cdot}001$). Tail I_{Ba} at -40 mV following a step to $+70$ mV from a holding potential of -80 mV was also reduced in axotomized neurones ($9{\cdot}7 \pm 0{\cdot}6$ nA for forty-two control neurones and $5{\cdot}2 \pm 0{\cdot}3$ nA for thirty-nine axotomized neurones; $P < 0{\cdot}001$). Minimal changes were observed in the kinetics of activation and deactivation.

3. Pharmacological experiments using 1,4-dihydro-2,6-dimethyl-3-nitro-4-(2-trifluoromethylphenyl)-pyridine-5-carboxylic acid methyl ester (BayK8644), nifedipine and ω-conotoxin showed that axotomy predominantly affected the N-type Ca^{2+} channels which carry the majority of I_{Ca} in these neurones. L-type Ca^{2+} current was little affected and T-type Ca^{2+} currents were not observed in control or axotomized cells.

4. Development of inactivation at 0 mV and recovery from inactivation of I_{Ba} at -80 mV exhibited three distinct components in both control and axotomized neurones: 'fast', 'intermediate' and 'slow'. The relative proportions of both the 'fast' and 'intermediate' components of inactivation at 0 mV were almost doubled after axotomy (fast component was 15% in control and 29% in axotomized neurones; intermediate component was 17% in control and 26% in axotomized neurones). 'Fast' and 'intermediate' inactivation tended to develop more rapidly and recover more slowly after axotomy. The rate of onset of 'slow' inactivation was unaffected by axotomy but the steady-state level at -40 mV was increased. Most of the change in I_{Ba} properties may be secondary to enhanced inactivation associated with axotomy.

* Permanent address: Faculty of Pharmacy, MRC Nerve Cell and Synapse Group, University of Toronto, Toronto, Ontario, M5S 2S2, Canada.

MS 1928

5. Axotomy reduced I_C (measured at the end of a 3 ms step from -40 to $+20$ mV) from $34{\cdot}5 \pm 4{\cdot}9$ ($n = 26$) to $19{\cdot}2 \pm 1{\cdot}5$ nA ($n = 49$, $P < 0{\cdot}005$). This reduction may be secondary to the reduction in calcium channels available for activation from -40 mV following axotomy.

6. The TTX-sensitive and TTX-insensitive components of peak Na^+ conductance (G_{Na}) were both increased after axotomy. Total G_{Na} was increased from $184{\cdot}9 \pm 8{\cdot}4$ to $315{\cdot}2 \pm 16{\cdot}4$ nS ($n = 37$ for both $P < 0{\cdot}001$). Most of the kinetic and steady-state properties of I_{Na} were unchanged after axotomy.

7. These results suggest that the increase in spike width produced by axotomy of bullfrog sympathetic neurones involves a decrease in I_{Ca} and consequent reduction in I_C. The complement of ion channels expressed after axotomy is quite unlike that which might be expected in 'immature' or 'dedifferentiated' neurones.

INTRODUCTION

Transection or damage to the axon of a central or peripheral neurone results in various morphological, biochemical and electrophysiological changes in the cell body (Lieberman, 1971; Titmus & Faber, 1990). This 'cell body reaction' has been interpreted as a reflection of the neurone's attempt to regenerate an axon (Grafstein & McQuarrie, 1978; but see also Carlsen, Kiff & Ryugo, 1982). If this is the case, one might expect that similar changes in neuronal properties would appear in all neuronal types as a consequence of the regenerative and degenerative mechanisms triggered by axotomy. This suggestion is difficult to reconcile with the observation that the effect of axotomy on action potential (AP) shape varies considerably according to neuronal type. For example, axotomy increases AP duration (spike width) in bullfrog sympathetic ganglion B-cells (Kelly, Gordon, Shapiro & Smith, 1986; Gordon, Kelly, Sanders, Shapiro & Smith, 1987) and in dorsal root ganglion cells of the cat cranial, carotid and glossopharyngeal nerves (Czeh, Kudo & Kuno, 1977; Gallego, Ivorra & Morales, 1987; Belmonte, Gallego & Morales, 1988) but not in hamster dorsal root ganglion cells (Gurtu & Smith, 1988). By contrast, axotomy decreases AP duration in guinea-pig vagal motoneurones (Laiwand, Werman & Yarom, 1988). Axotomy also produces a variety of changes in different neuronal types in the amplitude and duration of the after-hyperpolarization (AHP) which follows the AP (Titmus & Faber, 1990) whereas the rate of rise of the AP is increased in most cell types which have been studied (Gallego *et al.* 1987; Belmonte *et al.* 1988). Although different neuronal types express different complements of ion channels, the variation in the electrophysiological response to axotomy could be explained by the hypothesis that specific types of ion channels are always similarly affected during the 'cell body reaction'. This is because changes in AP configuration in a given cell type would reflect the relative abundance and importance of 'axotomy-sensitive' channels for AP generation. This hypothesis can only be tested by using voltage- and patch-clamp techniques to study specific ionic conductances in a variety of neuronal types. In the present work, we compared Ca^{2+}, Na^+ and K^+ currents from control bullfrog sympathetic B-neurones with those recorded from neurones 13–15 days after *in vivo* axotomy. Axotomy of these cells results in an increase in the width and height of the AP and a decrease in the amplitude and duration of the AHP (Kelly *et al.* 1986; Gordon *et al.* 1987). We tested whether the previously described increase in spike

width resulted from decreases in Ca^{2+} current and concomitant reduction of the voltage-dependent $G_{K,Ca}$ (Ca^{2+}-activated K^+ conductance) which repolarizes the AP (I_C; Adams, Brown & Constanti, 1982) or whether it resulted from slowing of I_{Na} inactivation.

Some of this work has previously appeared in abstract form (Jassar & Smith, 1991*a*, 1992).

METHODS

Small- to medium-sized bullfrogs (10–12 cm) were purchased from a biological supply house and stored in running water at room temperature (20 °C). The surgical procedures for axotomy of spinal nerves *in vivo* were carried out under aseptic conditions. The animals were anaesthetized by injecting a 2·5 % w/v solution of 3-aminobenzoic acid ethyl ester methanesulphonate salt (MS-222) into the dorsal lymph sac. The level of anaesthesia was deemed adequate when the animal failed to respond to a noxious stimulus (forceps pinch) applied to the hindlimb toe. Unilateral axotomy of spinal nerves (on the right side of each animal) was performed by excising 5–10 mm of the VIIIth, IXth and Xth (and sometimes VIIth) spinal nerves 5–10 mm below the Xth paravertebral ganglion. Nerves were exposed through a 1 cm dorsolateral incision in the body wall in the middle of the lumbar region. The incision was sutured using fine silk thread. Following recovery from anaesthesia, axotomized animals were maintained in tetracycline solution (0·16 g/l) in plastic tanks. This solution was changed on alternate days.

Controls (unoperated) and axotomized frogs were killed by decapitation and their spinal cords destroyed by 'pithing'. The VIIth–Xth paravertebral sympathetic ganglia were removed from both sides of each control animal or from the axotomized side of two axotomized animals and dissociated using the trypsin/collagenase procedure previously described (Jassar & Smith, 1991*b*). The dissociated cells were resuspended in fresh '6K external solution'. '6K external solution' contained (mM): NaCl, 113; KCl, 6; $MgCl_2$, 2; $CaCl_2$, 2; Hepes (acid), 5; and glucose, 10 (pH adjusted to 7·2 with NaOH). Cells were stored at about 5 °C until use and were sometimes washed with cold '6K external solution to remove any remaining enzymes. They were placed in a small plastic Petri dish under a Nikon 'Diaphot' inverted microscope and studied within 1–8 h after dissociation. 'Control' data were usually obtained from cells dissociated from the ganglia of unoperated frogs. Occasionally, ganglia from the unoperative side of axotomized frogs were used. Since there were no obvious differences between the currents recorded from these two control groups, the data from the two groups were pooled. Ba^{2+} was used as the charge carrier to study currents through Ca^{2+} channels. For these experiments, the 'external' solution contained (mM): *N*-methyl-D-glucamine (NMG) chloride, 117·5; NMG-Hepes, 2·5; $BaCl_2$, 2·0; (pH 7·2). 'Internal' solution consisted of (mM): NMG-Cl, 76·5; Hepes, 2·5; Tris–BAPTA, 10; Tris-ATP, 5; $MgCl_2$, 4 (pH 7·2; Jones & Marks, 1989*a*). For sodium currents, 'external' solution contained (mM): NaCl, 97·5; TEA-Br, 20; $MnCl_2$, 4; Tris-Cl, 2·5 (pH 7·2). The 'internal' solution contained (mM): CsCl, 103; NaCl, 9; TEA-Br, 5; Cs-Hepes, 2·5; Cs-EGTA, 1 (pH 7·2; Jones, 1987). To study I_C, 'external' solution contained: KCl, 2; $CaCl_2$, 4; NMG-Cl, 40; Tris-Cl, 2·5; sucrose, 134; D-glucose, 10. $CaCl_2$ was replaced with $MgCl_2$ in this external solution and 50 μM $CdCl_2$ was added to block Ca^{2+} influx which normally is responsible for activating I_C. 'Internal solution' contained (mM): KCl, 110; NaCl, 10; $MgCl_2$, 2; $CaCl_2$, 0·4;' EGTA, 4·4; Hepes, 5; D-glucose, 10; cyclic AMP, 0·125; leupeptin, 0·1 (pH 7·2). External solutions were 250 mosmol/kg and internal solutions were 240 mosmol/kg. The Petri dishes were superfused with external solutions at a flow rate of 2 ml/min. This flow rate allowed exchange of solutions within about 2 min. Drugs were applied by superfusion. All solutions containing dihydropyridines were administered under subdued lighting conditions from light-proof reservoirs. 1,4-dihydro-2,6-dimethyl-3-nitro-4-(2-trifluoromethylphenyl)-pyridine-5-carboxylic acid methyl ester (BayK8644) and nifedipine were dissolved in DMSO (dimethyl sulphoxide) to make 3 and 10 mM stock solutions, respectively. These solutions were diluted 1 in 10000 in external solution for application to ganglion cells.

Cells of intermediate size (usual input capacitance (C_{in}) 40–80 pF) were selected for recording. These were presumed to be B-cells (Dodd & Horn, 1983). An Axopatch 1B amplifier was used to record Ba^{2+} currents (I_{Ba}) and data collection usually started 15 min after establishing whole-cell recording conditions. Series resistance measured following break-through was 3–12 MΩ (usually 5–8 MΩ). Data were analysed only from cells in which there was no run-down of I_{Ba} within the

first 15 min of data collection. In such cells, the amplitude of I_{Ba} was 60–80% of its original value even after 75 min of recording. To limit reduction in successive responses due to slow I_{Ba} inactivation (Jones & Marks, 1989*b*), the interval between successive depolarizing voltage commands was 15 s and the interval between successive experimental protocols was at least 3 min (Jassar & Smith, 1991*b*). Cells were held at −80 mV during these intervals. Series resistance compensation was monitored and readjusted throughout the experiment (always at 80%). The error in clamp potential in recording a current of 6 nA, due to series resistance of 8 MΩ at 80% compensation, would be approximately 10 mV. This would reflect a maximum error for peak Ba^{2+} currents which was < 6 nA. Greater voltage errors would be expected for the larger I_{Ba} tail currents. Cancellation of capacity transients and leak subtraction was done by applying 25% amplitude hyperpolarizing pulses, multiplying responses by four and addition (Jones & Marks, 1989*a*). Membrane capacitance was compensated at the start of recording and C_{in} was estimated by reading the dial used to compensate the capacitance. Whole-cell capacitance compensation was disabled prior to data collection.

I_{Na} and I_C were recorded using an Axoclamp 2A amplifier in the single-electrode, discontinuous voltage-clamp mode (Jones, 1987). These currents, which were typically > 20 nA, are too large to study with the Axopatch 1B amplifier. Also, the use of a 'switching amplifier' minimizes series-resistance problems associated with large, rapidly activating currents because the amplifier headstage is clamped to the recorded membrane voltage and the electrode itself does not contribute to the series resistance. Using low-resistance patch electrodes coated with 'Sigmacote' (Sigma, St Louis, MO, USA), it was possible to achieve switching frequencies between 35 and 55 kHz (usually 45–50 kHz) and a clamp gain between 12 and 25 nA/mV (usually 16–20 nA/mV). The steady-state voltage error (V_S) reported by an electrode in recording 30 pA current from a 70 pF cell with a clamp gain of 16 nA/mV and a switching frequency of 45 kHz will be < 1 mV, as estimated from the equation

$$V_S = I/gFC_{in},$$

where I = current, g = clamp gain , F = switching frequency and C_{in} = whole-cell capacitance (Finkel & Redman, 1984; Jones, 1987). Peak clamp voltage error (V_E) is given by the expression

$$V_E = I(d/FC_{in}),$$

where d = 1 − 'duty cycle' (= 0·7 for Axoclamp 2A). For a 30 nA current recorded from a 70 pF cell using a 45 kHz switching frequency, the error would be 6·7 mV.

Data were digitized using a Labmaster DMA interface and stored on an IBM-compatible computer (Northgate 386) fitted with removable hard disc systems (Bernoulli drive, Iomega, Corp., Roy, UT, USA). During data acquisition, the corner frequency of the filter was set to 5 kHz for I_{Ba} and the bandwidth of the filter was 10 or 30 kHz for I_{Na} and I_C. Permanent records were made from the hard disc using an X–Y plotter. Data were acquired and analysed using 'PCLAMP' software (Axon Instruments, Burlingame, CA, USA). Tail current amplitudes were measured at 500 μs (for I_{Ba}) or at peak amplitude of the tail (for I_C) after the termination of a command pulse following subtraction of capacity currents. This procedure seemed appropriate for estimating the peak amplitudes of the relatively slow tail currents which would flow at the test potential of −40 mV (see Fig. 1). All data are presented as means ± S.E.M. In graphs where no error bars are visible, the error bars are smaller than the symbols used to designate the data points.

All drugs and chemicals were purchased from Sigma (St Louis, MO, USA) except for Bay K 8644 and nifedipine which were gifts from Dr Susan Dunn.

RESULTS

All data on the effects of axotomy were obtained 13–15 days after section of the postganglionic nerves. Axotomy-induced changes in the AP characteristics of bullfrog sympathetic ganglion cells seem to be maximal at this time (Gordon *et al.* 1987).

Effects of axotomy on I_{Ba}

Figure 1 illustrates I_{Ba} evoked in a control and in an axotomized neurone following a series of depolarizing voltage commands from a holding potential of −80 mV. I_{Ba}

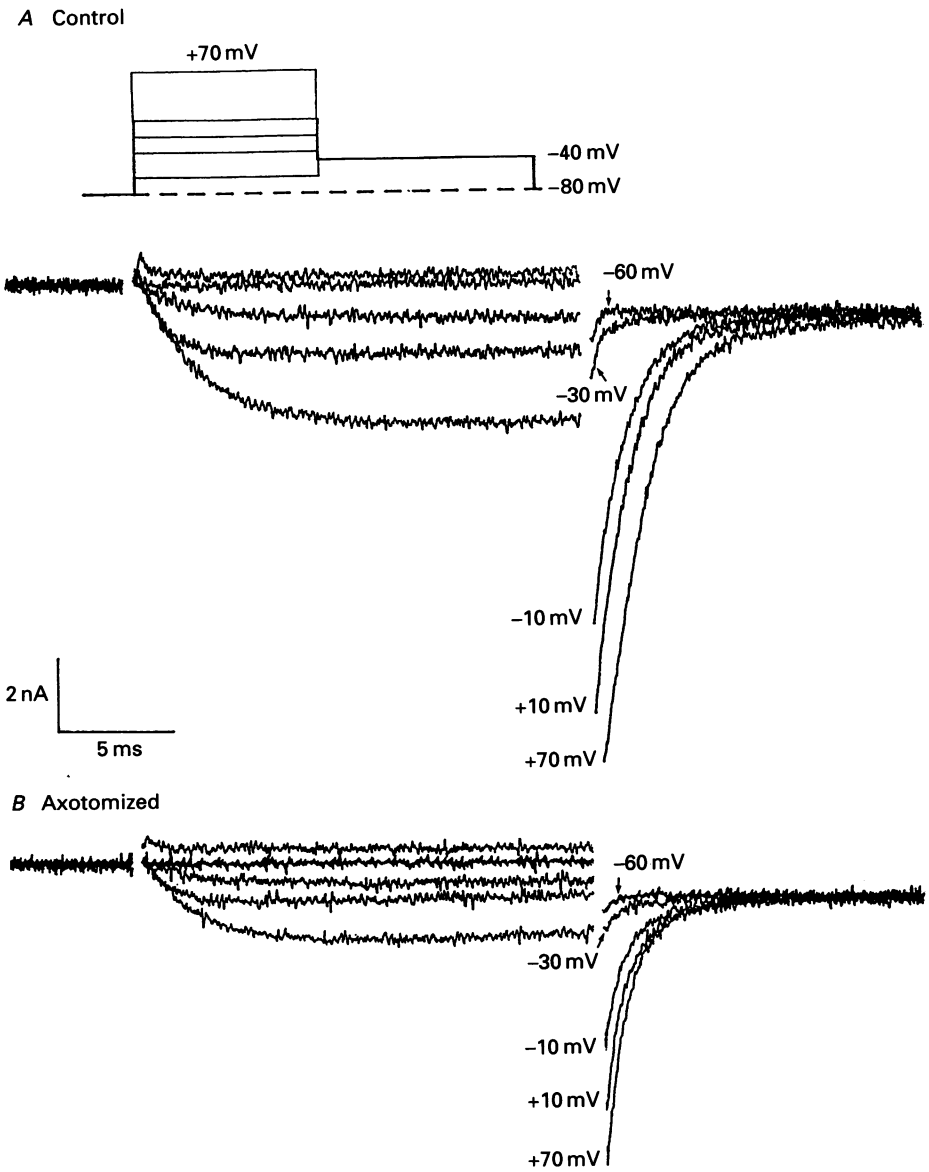

Fig. 1. Effects of axotomy on Ba^{2+} currents. *A*, voltage protocol and a family of I_{Ba}s evoked from a typical control neurone. Cell was held at −80 mV and stepped to different depolarizing potentials for 20 ms and then stepped back to −40 mV. *B*, a family of I_{Ba}s evoked from a typical axotomized neurone using the same protocol as for the cell in *A* (288 μs are blanked at the beginning and at the end of the depolarizing command pulse). Note decrease in peak and tail current amplitude after axotomy.

tails (at −40 mV) were recorded at the end of each depolarizing pulse. The current in the axotomized cell is obviously much smaller than that recorded in the control neurone. Figure 2*A* illustrates the average *I–V* relationship obtained from peak I_{Ba}

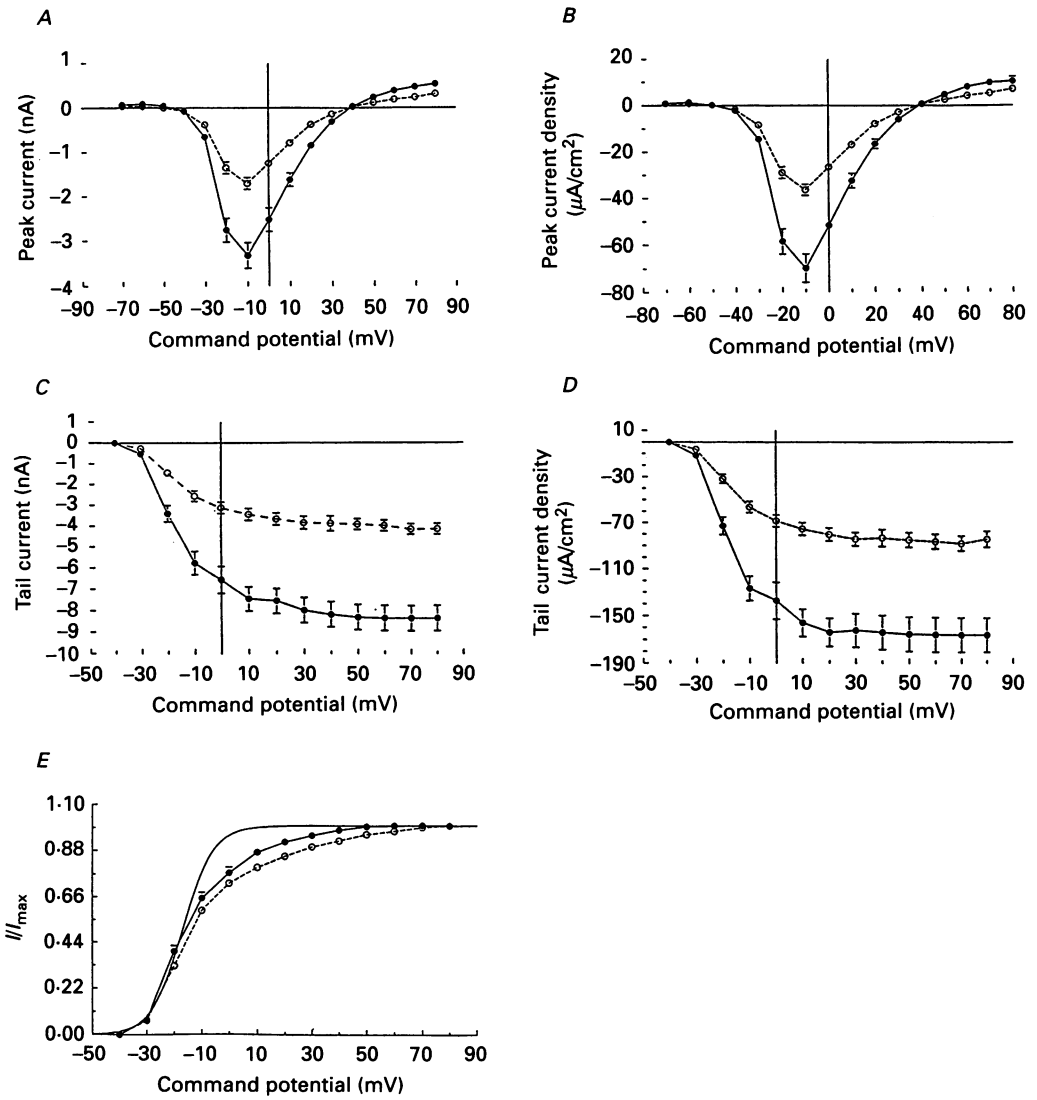

Fig. 2. Comparison of I_{Ba} in control and axotomized neurones. *A*, current–voltage relationship for peak I_{Ba} from forty-two control (●) and thirty-nine (○) axotomized cells. *B*, data from cells used in *A* replotted as current density–voltage relationship. Current density was calculated from C_{in} assuming a specific membrane capacitance of 1 μF/cm^2. *C*, current–voltage relationship for tail I_{Ba} current from forty-two control (●) and thirty-nine axotomized (○) cells. *D*, data from cells used in *C* replotted as current density–voltage relationship as in *B*. *E*, normalized tail current amplitudes from control and axotomized cells plotted as a function of command potential. Symbols represent the observed data points and the continuous line is a plot of the Boltzmann equation of the form

$$I_{t(V)}/I_{t(\max)} = G_V/G_{\max} = \{1+\exp^{ze(V_0-V)/kT}\}^{-1},$$

where $I_{t(V)}$ is the amplitude of the I_{Ba} tails following a command to voltage V, and $I_{t(\max)}$ is the maximum amplitude of I_{Ba} tails seen following commands to positive voltages. The ratio of these currents is equal to the ratio of Ba^{2+} conductances $G_V/G_{\max}$ which is an index of the fraction of Ca^{2+} channels open. z = valency of the gating particle, e = elementary electronic charge ($1{\cdot}602 \times 10^{-19}$ C), k = Boltzmann's constant ($1{\cdot}381 \times 10^{-23}$ V C K^{-1}), T = absolute temperature and V_0 is the potential for half-maximal activation.

in forty-two control and thirty-nine axotomized cells (13–15 days after axotomy). Axotomy reduced peak I_{Ba} at -10 mV from $3{\cdot}3 \pm 0{\cdot}3$ ($n = 42$) to $1{\cdot}7 \pm 0{\cdot}1$ nA ($n = 39$, $P < 0{\cdot}001$). Figure 2*C*, which illustrates the average tail current amplitudes from forty-two control and thirty-nine axotomized cells, gives a measure of the extent of I_{Ba} activation by the various voltage commands in control and axotomized cells. This reduction in peak I_{Ba} and in I_{Ba} tails was also obvious when the data were replotted as current densities (Fig. 2*B* and *D*) and suggests that our selection of cells within a particular range of diameters minimized the variability of the total current which could result from differences in cell size. This observation justifies the use of raw current amplitude for comparison of data for other currents between control and axotomized cells reported in this study. The mean data points from Fig. 2*C* have been normalized and replotted in Fig. 2*E*. The continuous line in Fig. 2*E* describes a Boltzmann equation in which z was set to 4·6 and V_0 to -17 mV. The line corresponds well to both axotomized and control data only at relatively negative potentials (see figure legend). The deviation at more positive membrane potentials probably reflects fast inactivation which develops during 20 ms test pulses. Inactivation is most pronounced between -40 and 0 mV and is reduced at $+70$ mV (see Fig. 7*D* and *E*; Jones & Marks, 1989*b*).

Pharmacology of Ba^{2+} currents before and after axotomy

Although single-channel conductances characteristic of both N- and L-type Ca^{2+} channels have been described in bullfrog sympathetic ganglion B-cells (Lipscombe, Madison, Poenie, Reuter, Tsien & Tsien, 1988), it has been reported that less than 10% of the channels are of the L-type (Jones & Marks, 1989*a*; Jones & Jacobs, 1990; Elmslie, Kammermeier & Jones, 1992). The effect of the N-type Ca^{2+} channel blocker, ω-conotoxin GVIA on whole-cell I_{Ba} was examined to test whether the proportion of L- to N-type current changed after axotomy. Some typical data records illustrating the reversible inhibition of I_{Ba} in a control neurone by 200 nM ω-conotoxin are shown in Fig. 3*A* (cf. Morrill, Boland & Bean, 1991). The effect of the toxin on the *I–V* relationship of fourteen control cells is shown in Fig. 3*B* and in fourteen axotomized cells in Fig. 3*C*. In control neurones at -10 mV, ω-conotoxin reduced the peak I_{Ba} to $1{\cdot}7 \pm 0{\cdot}1$ nA ($n = 14$) and after axotomy to $1{\cdot}4 \pm 0{\cdot}1$ nA ($n = 14$). Thus, there was little or no change in the amount of ω-conotoxin-resistant current remaining after axotomy ($0{\cdot}1 > P > 0{\cdot}05$). This point is illustrated further by the data in Fig. 3*D* which shows the time course of the effect of ω-conotoxin on I_{Ba} (at -10 mV) in control and axotomized neurones. In both situations, the inhibition of the current takes 20–25 min to reach a steady state and the effect is almost completely reversed after about 1 h. Although the toxin reduces I_{Ba} (at -10 mV) to $26{\cdot}5 \pm 1{\cdot}4$% in control cells and to $38{\cdot}5 \pm 2{\cdot}5$% in axotomized cells, there is more total current in the control neurones than in the axotomized neurones and the amount of ω-conotoxin-resistance current is unchanged. It is possible that 200 nM ω-conotoxin did not produce a maximal effect as Elmslie *et al.* (1992) reported only 7 ± 2% of resistant I_{Ba} in 1 μM conotoxin.

If some of this ω-conotoxin-resistant fraction of the total current is carried by L-type channels (Jones & Marks, 1989*a*; Jones & Jacobs, 1990) dihydropyridines would be expected to affect the total I_{Ba} by the same absolute amount in both control and axotomized neurones. Nifedipine (1 μM) failed to affect I_{Ba} in control or

axotomized cells whereas the current was potentiated in both situations by Bay K 8644 (300 nM). The additional amount of current seen in control neurones at −20 mV (2·5±0·4 nA; $n = 11$) was similar to that seen in axotomized cells (1·7±0·5 nA, $n = 12$; $P > 0·2$). This was accompanied by a shift in the activation

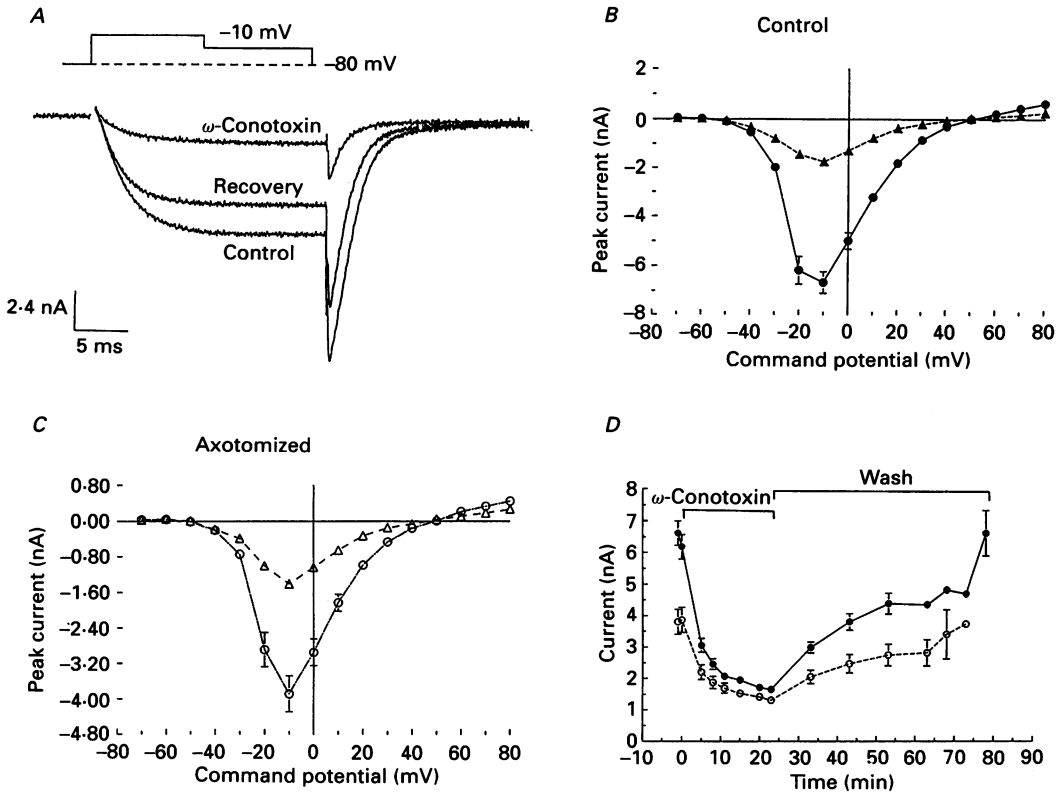

Fig. 3. Comparison of effect of 200 nM ω-conotoxin on I_{Ba} in control and axotomized neurones. *A*, typical data records from a control neurone showing reversible blockade of I_{Ba}. *B*, *I–V* relationship for I_{Ba} in control neurones ($n = 14$) in the presence (▲) and absence (●) of 200 nM ω-conotoxin. *C*, *I–V* relationship for I_{Ba} in axotomized neurones ($n = 14$) in the presence (△) and absence (○) of 200 nM ω-conotoxin. *D*, time course of the effect of ω-conotoxin and recovery from the effect of ω-conotoxin in control (●) and axotomized (○) neurones. Holding potential = −80 mV.

curve to more hyperpolarized potentials. When the solution containing Bay K 8644 was replaced by one containing 1 μM nifedipine, I_{Ba} was reduced to levels less than its initial value in control and axotomized cells at all voltages. Nifedipine after Bay K 8644 reduced the control I_{Ba} at −10 mV by 1·9±0·1 nA ($n = 11$) in control cells, and by 1·5±0·3 nA ($n = 12$) ($P > 0·2$) after axotomy. Again, there was no difference in the amount of current affected. Typical data records for currents activated in a control cell at 0 and −20 mV are shown in Fig. 4*A a* and *A b*. The *I–V* plots for eleven control and twelve axotomized cells (Fig. 4*B* and *C*) show the potentiation of I_{Ba} by Bay K 8644 and its subsequent suppression by nifedipine. The

potentiation produced by BayK8644 was most apparent at potentials negative to −20 mV whereas the depression produced by nifedipine was most apparent at potentials positive to −20 mV. This effect is also quite evident from the data records illustrated in Fig. 4*Aa* and *Ab*. These effects of dihydropyridines and ω-conotoxin suggest that axotomy predominantly affects N-type and not L-type Ca^{2+} channels.

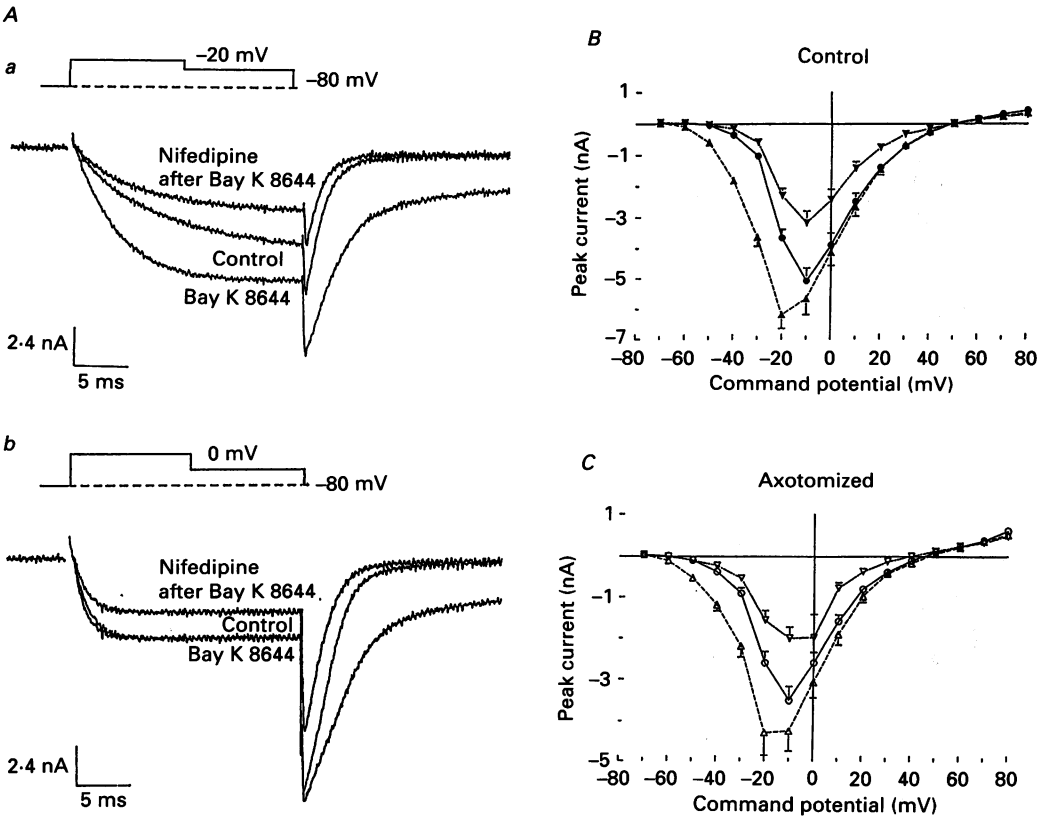

Fig. 4. Voltage dependence of the effects of dihydropyridines on I_{Ba} in control and axotomized neurones. *Aa*, BayK8644 (300 nM) potentiates I_{Ba} evoked by stepping from −80 to −20 mV and subsequent application of nifedipine (1 μM) reduces the potentiated current to less than the initial level. *Ab*, BayK8644 (300 nM) does not potentiate I_{Ba} evoked by stepping from −80 to 0 mV but subsequent application of nifedipine (1 μM) still reduces the current to less than the control value. Traces in *a* and *b* were obtained from a control neurone. *B*, *I–V* relationship for I_{Ba} in control neurones ($n = 11$) prior to the addition of dihydropyridines (●), in the presence of BayK8644 (▲) and in the presence of nifedipine (after exposure to BayK8644) (▼). *C*, *I–V* relationship for I_{Ba} in axotomized neurones ($n = 12$) prior to the addition of dihydropyridines (○), in the presence of BayK8644 (△) and in the presence of nifedipine (after exposure to Bay K8644) (▽). Holding potential = −80 mV.

Effects of axotomy on inactivation of I_{Ba}

To investigate the effects of axotomy on steady-state inactivation properties, I_{Ba} was evoked from three different holding potentials of −90, −60 and −40 mV

(Fig. 5). The I–V relationship for peak I_{Ba} clearly shows that shifting the holding potential from -60 to -90 mV has a larger effect on peak I_{Ba} in the axotomized cells than in the control cells. After axotomy, such a shift in holding potential almost doubles I_{Ba} at -10 mV (from $0{\cdot}85 \pm 0{\cdot}11$ nA, $n = 8$, to $1{\cdot}75 \pm 0{\cdot}12$ nA, $n = 8$,

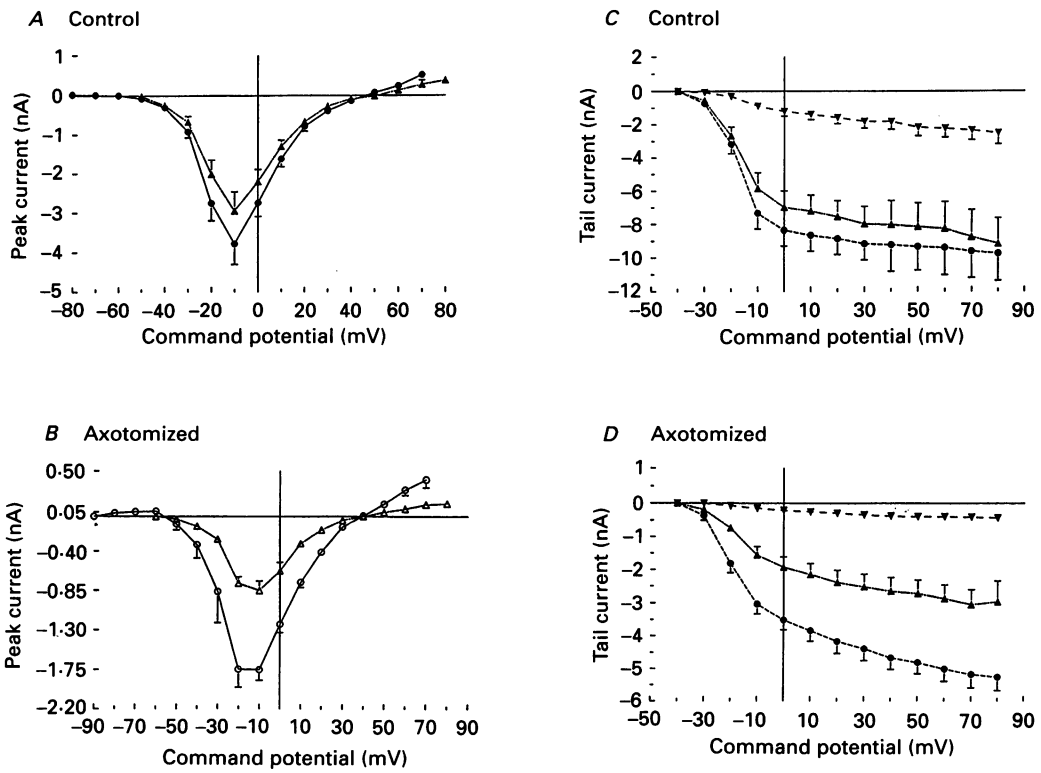

Fig. 5. Effects of axotomy on I_{Ba} evoked from different holding potentials. *A*, I–V relationship for I_{Ba} evoked from holding potentials of -90 mV (●) and -60 mV (▲) for eight control cells. *B*, I–V relationship for I_{Ba} evoked from -90 mV (○) and -60 mV (△) for eight axotomized cells. *C*, I–V relationship for tail I_{Ba} evoked from -80 mV (●), -60 mV (▲) and -40 mV (▼) for eight control cells. *D*, I–V relationship for tail I_{Ba} evoked from -80 mV (●), -60 mV (▲) and -40 mV (▼) for eight axotomized cells.

$P < 0{\cdot}001$; Fig. 5*B*), whereas in the control situation changing the holding potential has little effect on I_{Ba} recorded at -10 mV ($0{\cdot}3 > P > 0{\cdot}2$; Fig. 5*A*). This effect is attributable to increased slow inactivation in axotomized neurones (see below). Figure 5*C* and *D* illustrates the I–V relationship for I_{Ba} tails (at -40 mV) evoked from different holding potentials from control and axotomized neurones. Changing the holding potential has a far stronger effect on the relative amplitude of I_{Ba} tails in axotomized neurones than in control neurones. Assuming that inactivation is negligible at -80 mV in both control and axotomized neurones, the effect of holding potential on I_{Ba} tails following a 20 ms pulse to $+70$ mV suggests that the mid-point voltage for inactivation is shifted from -48 to approximately -58 mV after axotomy (cf. Jones & Marks, 1989*b*). The assumption of negligible inactivation at

−80 mV in axotomized neurones may be incorrect. Tail currents carried by Ba^{2+} at −40 mV following a 20 ms step command to +70 mV from a holding potential of −80 mV are reduced by 41% in axotomized neurones (9·2±1·2 nA in control neurones, Fig. 5*C*; 5·4±0·4 nA in axotomized neurones, Fig. 5*D*). Our observations could equally well indicate that the mid-point voltage for inactivation was in fact shifted to about −76 mV after axotomy and that the number of calcium channels is not in fact changed by axotomy. If this were the case, the increase in slow inactivation with depolarization would have to change from about *e*-fold per 7 mV to about *e*-fold per 14 mV in axotomized neurones.

Figure 6 illustrates the onset and recovery from inactivation of I_{Ba} following a 1 s conditioning pulse to 0 mV. The experimental protocol and typical current records from a control and an axotomized neurone are illustrated in Fig. 6*A*. The current remaining at the end of the 1 s pulse was 64±2% in control neurones (36±2% inactivation; $n = 39$) and 40±2% (60±2% inactivation; $n = 35$) for axotomized neurones. I_{Ba} evoked by 1 s pulses to 0 mV from a holding potential of −80 mV shows two components of inactivation: 'fast' and 'intermediate'. The contribution of these two components was quantified by fitting the decay phase to the sum of two exponential components plus an offset and the data are summarized in Table 1. The amplitude of the 'fast' inactivating component (A_1) contributes 15±2% of total I_{Ba} evoked in control cell ($\tau_1 = 58 \pm 4$ ms; $n = 26$) and 29±2% for axotomized neurones ($\tau = 45 \pm 2$ ms; $n = 35$). The extrapolated values of the amplitude of the 'intermediate' component (A_2) comprised 40±2% of total I_{Ba} in control neurones ($\tau_2 = 746 \pm 30$ ms) and 44±1% in axotomized neurones ($\tau_2 = 479 \pm 15$ ms). When these 1 s pulses were evoked every 15 s, there was decrement of current between successive responses. This decrement appears to be due to build-up of a 'slow' form of inactivation In Fig. 6*B* the normalized peak I_{Ba} is plotted against pulse number. The data can be described by an exponential approach to a new steady-state value. The rates of onset (k_+) and recovery (k_-) of slow inactivation can be estimated from the parameters describing the decrement (see Appendix). If x is the steady-state fractional decrement due to 'slow' inactivation and $1/\lambda$ is the number of pulses required to reach e^{-1} of this steady-state value then

$$(1-x)\,k_+ \times 1 \text{ s} = x\,k_- \times 15 \text{ s},$$

and

$$\lambda = (k_+ \times 1 \text{ s}) + (k_- \times 15 \text{ s}).$$

Thus, knowing the values of λ and the steady-state decrement one can derive k_+ and k_-. The extrapolated steady-state decrement was 49% for control cells and 37% for axotomized cells. The values of λ estimated from Fig. 6*B* were 0·091 for control cells and 0·108 for axotomized cells. The derived values of k_+ and k_- are 0·043 and 0·0031 s^{-1} in control, and 0·041 and 0·0045 s^{-1} in axotomized neurones. These values yield the time constants for onset (at 0 mV) and offset (at −80 mV) of the 'slow' component of inactivation (τ_3) in Table 1. The value of τ_3 of around 4–5 min at −80 mV agrees well with the data of Jones & Marks (1989*b*) and is consistent with the frequency-dependent inactivation described by Jassar & Smith (1991*b*). Figure 6*B* also shows that a single 1 s pulse is associated with about 6% slow inactivation (A_3).

Once the 'fast' and 'slow' components of the total inactivation during the 1 s

pulse are accounted for, the total inactivation observed at the end of the pulse relative to the peak suggests that 17 and 26% 'intermediate' inactivation developed during the 1 s pulse in control and axotomized cells respectively (see Table 1 for details). However, using the time constants and extrapolated amplitude of the

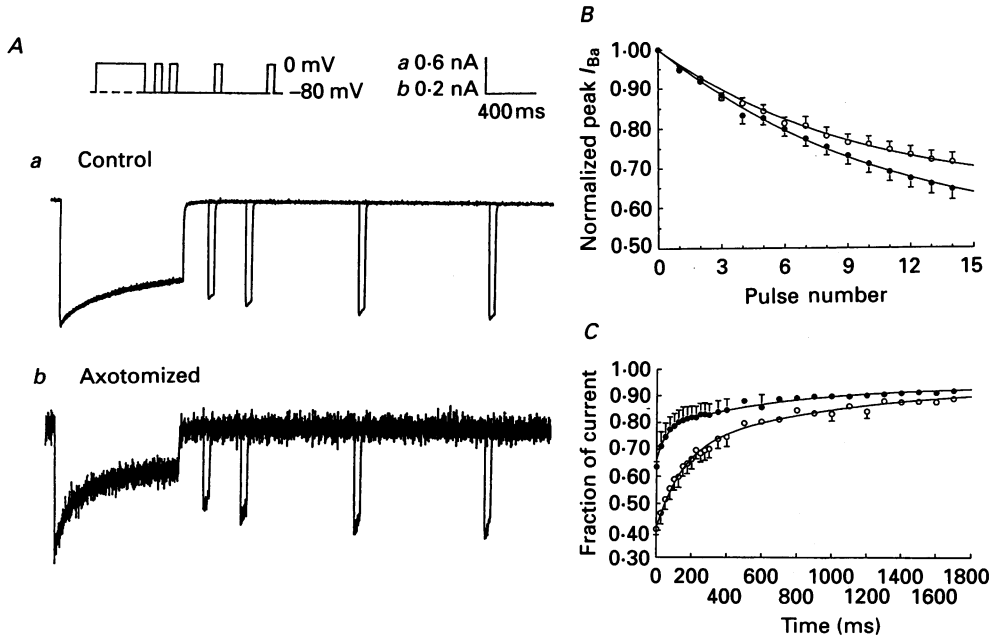

Fig. 6. Effects of axotomy on time dependence of onset and recovery from inactivation. *A*, cells were stepped to 0 mV for 1 s from a holding potential of −80 mV during the conditioning pulse followed by a 75 ms test pulse to 0 mV applied at increasing intervals from 25 to 1700 ms every 15 s (0·66 Hz). *Aa* and *Ab*, I_{Ba} was evoked using the voltage protocols illustrated in the upper panel from a control and an axotomized neurone, respectively. The amplitudes of the currents evoked in successive pulses have been scaled to superimpose exactly the currents evoked during the conditioning pulse in the first trial for comparison. The calibration for current amplitude is correct for the first pulse only. *B*, onset of 'slow' inactivation of I_{Ba} (at 0 mV) in control (●) and axotomized (○) neurones. The peak I_{Ba} during each 1 s conditioning pulse is normalized to the peak I_{Ba} observed during the first 1 s conditioning pulse and plotted against the pulse number. Continuous lines through the data describe the relative decrement of current between successive pulses for the control cells by the equation $I(n)/I(0) = 0{\cdot}51 + (0{\cdot}49)\exp^{-0{\cdot}091n}$ and by the expression $I(n)/I(0) = 0{\cdot}63 + (0{\cdot}37)\exp^{-0{\cdot}108n}$ for axotomized cells, where $I(n)$ refers to the peak I_{Ba} evoked in the nth conditioning pulse and $I(0)$ refers to peak I_{Ba} evoked in the first pulse of the train and n is the pulse number, the first one designated as 0. *C*, rate of recovery from inactivation (at −80 mV) measured from the amplitude of 75 ms test pulses in control (●) and axotomized (○) neurones. Continuous lines are plots of the equation $I_0/I_{0(max)} = 1 - (0{\cdot}06\exp^{-0{\cdot}0000031t}) - (0{\cdot}16\exp^{-0{\cdot}0013t}) - (0{\cdot}12\exp^{-0{\cdot}020t})$ for control data and by $I_0/I_{0(max)} = 1 - (0{\cdot}06\exp^{-0{\cdot}0000045t}) - (0{\cdot}25\exp^{-0{\cdot}0010t}) - (0{\cdot}28\exp^{-0{\cdot}0070t})$ for axotomized data where I_0 is peak I_{Ba} during test pulse, $I_{0(max)}$ is peak I_{Ba} during conditioning pulse and t is the delay between the conditioning and test pulses.

'intermediate' component estimated from the fits of the decay of I_{Ba} and subtracting the 'slow' component one predicts 24 and 30% intermediate component in control and axotomized neurones respectively. It is likely that the pulse duration (1 s) is not

long enough to define accurately the 'intermediate' component. Using 3 s pulses, a 1·5 s time constant is observed in the inactivation of I_{Ba} (Wertz, Elmslie & Jones, 1993).

The three components of inactivation are also apparent in the kinetics of recovery (Fig. 6*C*). These were determined using a test pulse of which the amplitude is

TABLE 1. Components of inactivation of I_{Ba}

		Total in 1 s (%)	A_1 (%)	τ_1 (ms)	A_2 (%)	τ_2 (ms)	A_3 (%)	τ_3 (s)
Onset at 0 mV	Control	44±2*	15±2	58±4	40±2	746±30	—	23§
	Axotomized	68±2*	29±2	45±2	44±1	479±15	—	25§
Recovery at −80 mV	Control	36±2†	12	50	16	746	6‡	326§
	Axotomized	60±2†	28	143	25	1000	6‡	220§

For onset of inactivation at 0 mV the values for time constants and relative amplitudes were obtained by fitting two exponential components plus an offset to the decay of the current during the 1 s pulse. A similar analysis was applied to average data for recovery from inactivation at −80 mV (see Fig. 6*C* and legend). '*A*' refers to percentage amplitude of the intercept and 'τ' refers to time constant. Subscripts 1, 2 and 3 refer to 'fast', 'intermediate' and 'slow' components of inactivation respectively.

* Estimated using values of A_1, τ_1, A_2 and τ_2 derived from biexponential fits to the inactivation during 1 s commands to 0 mV from −80 mV.

† Determined from the ratio of amplitudes of I_{Ba} at the end of the 1 s pulse over the peak I_{Ba} for the pulse.

‡ Determined from the decrement of the peak I_{Ba} between successive pulses.

§ Estimated from decrement of peak I_{Ba} during 0·067 Hz train of 1 s commands to 0 mV.

expressed as a fraction of the peak of the corresponding conditioning pulse. The amplitudes of the 'fast', 'intermediate' and 'slow' components observed during recovery appear to correspond to those observed during onset of inactivation.

Table 1 illustrates that axotomy increases both 'fast' and 'intermediate' components of inactivation. Onset of slow inactivation at 0 mV and recovery at −80 mV do not appear to be affected much. It should be recalled, however, that Fig. 5 suggests that some form of 'slow' inactivation is enhanced in axotomized neurones such that the half-inactivation voltage is shifted from −48 mV to at least −58 mV after axotomy. Thus, the similarity in time constants of inactivation at 0 mV and −80 mV may be coincidental. More experiments using different test potentials will be required to explore the voltage dependence of slow inactivation.

The effects of axotomy on voltage dependence of 'fast' inactivation of I_{Ba} were studied using a voltage protocol which involved a 500 ms conditioning pulse followed by a 75 ms test pulse (Jones & Marks, 1989*b*). Typical traces are illustrated in Fig. 7*A*. Maximal peak I_{Ba} flows during conditioning pulses to −10 or −20 mV and this current displays obvious decrement by the end of the 500 ms conditioning pulse which is more pronounced in the axotomized neurone (Fig. 7*Ab*). Percentage inactivation of I_{Ba} (at −10 mV) during a 500 ms depolarizing pulse was 29·6±2·2 in control neurones ($n = 44$) and 46·8±1·6 in axotomized neurones ($n = 57$; $P < 0·001$). Figure 7*B* shows that the current available for activation in the 75 ms test pulse is minimal when the conditioning pulse is associated with maximal current (i.e.

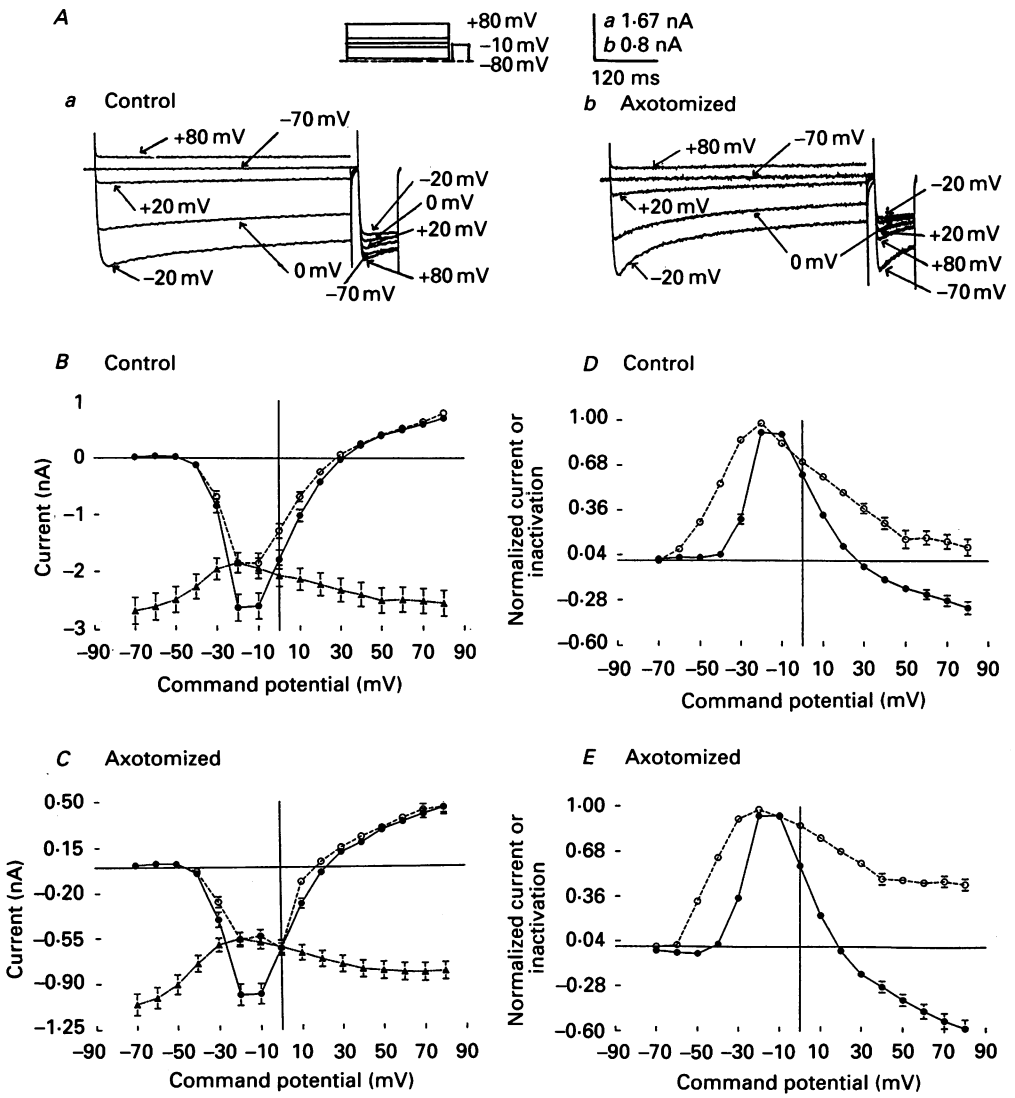

Fig. 7. Effects of axotomy on voltage dependence of inactivation of I_{Ba}. *A*, voltage protocol and series of current responses from a control neurone (*a*) and axotomized neurone (*b*). Each conditioning step from the holding potential of −80 mV to a depolarized potential was followed by a 'test' pulse to −10 mV. Calibration *a* refers to control records (*a*) and calibration *b* refers to records from the axotomized cell (*b*). Note that the smaller currents in the axotomized neurone inactivate to a greater extent and have a higher rate of inactivation as compared to those in the control neurone. *B*, peak (●), end of pulse (○) and test pulse current (▲) from forty-four control neurones plotted as a function of the command potential used for the conditioning pulse. *C*, peak (●), end of pulse (○) and test pulse current (▲) from fifty-seven axotomized neurones plotted as a function of the command potential in the conditioning pulse. *D*, data from control neurones (*B*, $n = 44$) normalized and replotted. Maximum peak current flowing during the conditioning pulse was defined as 1 for each cell and peak current at different depolarizing potentials (●) normalized to this value. Minimum current elicited for each cell for a test pulse (to −10 mV) was taken as maximum inactivation (= 1) and other values were

maximal inactivation is seen following pulses to −10 or −20 mV). Inactivation is reduced at positive potentials where I_{Ba} is reduced. This result is suggestive of 'current-dependent' inactivation. However, significant inactivation is observed at −50 mV where little I_{Ba} is apparent. Jones & Marks (1989*b*) have suggested that the current dependence is only apparent and, in fact, represents the voltage-dependence of inactivation such that less inactivation develops at positive potentials. Figure 7*C* illustrates the data for inactivation of I_{Ba} from fifty-seven axotomized neurones. A more convenient method of illustrating inactivation in control and axotomized cells is shown in Fig. 7*D* and *E*. Currents recorded during the conditioning pulses were normalized to their maximum values and plotted against voltage. Minimum current during test pulses was defined as maximum inactivation. Inactivation at various potentials was normalized to this value. This yields a more direct comparison of conditioning current amplitude and the amount of inactivation (cf. Jones & Marks, 1989*b*). The data illustrate that the enhanced inactivation seen in axotomized neurones is especially apparent at positive potentials ($P < 0{\cdot}001$ for voltages from 0 to +50 mV).

Unlike the data presented in Figs 2 and 3, currents illustrated in Fig. 7 were not leak-subtracted. The apparent reversal potential for I_{Ba} in control cells (Fig. 7*B* and *D*) is more positive than that for axotomized cells (Fig. 7*C* and *E*). This difference may result from a greater contribution of outward leak current in axotomized cells because it is opposed by a weaker inward I_{Ba} under these conditions. Leak current is not altered by axotomy (B. S. Jasar, P. S. Pennefather & P. A. Smith, submitted).

Effects of axotomy on activation and deactivation of I_{Ba}

The kinetics of activation and deactivation of I_{Ba} were examined to further explore any changes in the properties of Ca^{2+} channels which might be induced by axotomy. Figure 8*A* illustrates the voltage dependence of the rate of activation and deactivation of I_{Ba}. Activation time constants (τ_{act}) were obtained by applying single-exponential fits to currents recorded from experiments such as that illustrated in Fig. 1 ($n = 42$ for control cells and $n = 39$ for axotomized cells). Deactivation time constants (τ_{deact}) were obtained from single-exponential fits to tail currents recorded at various potentials following a step command to −10 mV ($n = 17$ for control cells and $n = 16$ for axotomized cells). An experiment of this type is illustrated in Fig. 8*B*. The difference in magnitude of deactivation and activation time constants at −30 mV (Fig. 8*A*) and the initial delay in activation of I_{Ba} (Fig. 8*B*) may indicate that multiple closed states precede opening of Ca^{2+} channels (Sala, 1991). Axotomy appears to increase the rate of I_{Ba} activation at relatively negative potentials (e.g. at −20 mV, $P < 0{\cdot}005$) whereas at more positive voltages (e.g. +30 mV), little or no effect could be detected ($P > 0{\cdot}6$). After axotomy, the rate of deactivation at −30 mV appeared to be increased ($P < 0{\cdot}02$) yet axotomy seemed to have little effect at more hyperpolarized membrane potentials ($P > 0{\cdot}2$ at −60 mV). Given the amplitude (≈ 13 nA, Fig. 8*B*) and time course of I_{Ba} tail currents (< 2 ms at

normalized to this value to give an index of inactivation (○). *E*, data from axotomized neurones (*C*) normalized and replotted for conditioning pulse current (●) and inactivation (○; $n = 57$).

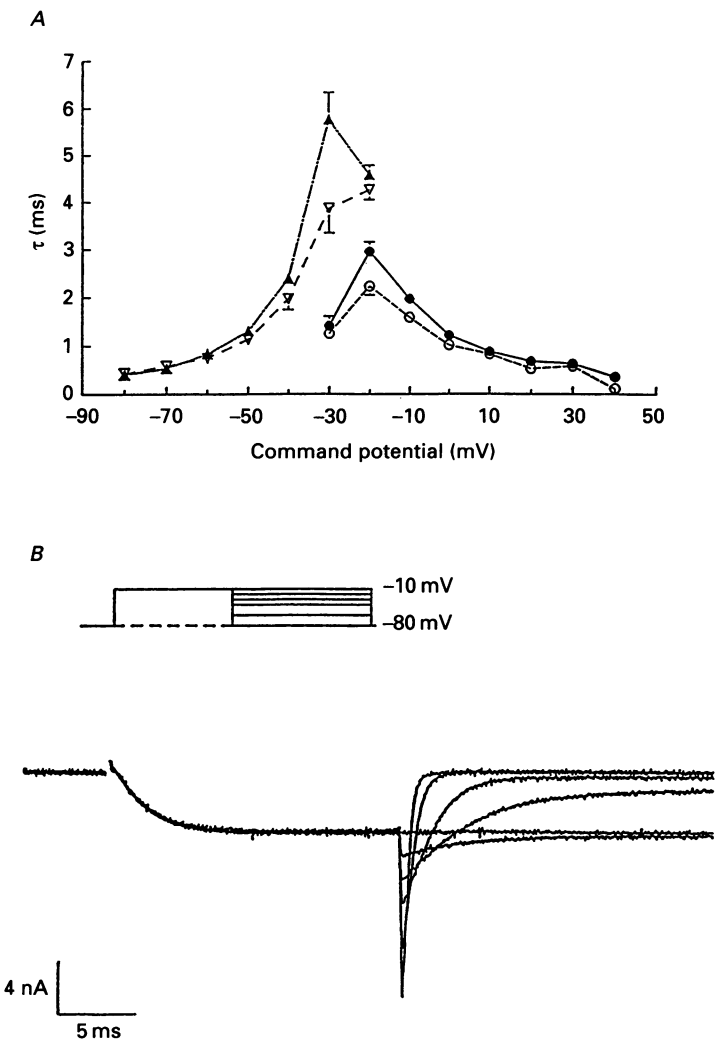

Fig. 8. Effects of axotomy on kinetics of activation and deactivation of I_{Ba}. *A*, voltage dependence of τ for activation (for control, $n = 42$, ●); and for axotomized, $N = 39$, ○) and deactivation (for control, $n = 14$, ▲; for axotomized, $n = 15$, ▽). τ_{act} (time constant of activation) was measured by fitting single-exponential curves to currents evoked by using the protocol shown in Fig. 1. *B*, upper panel shows voltage protocol for studying deactivation. Cells were stepped to −10 mV for 20 ms and then stepped back to a series of less-depolarized potentials to observe tail currents. Lower panel shows a family of I_{Ba}s and tail currents evoked from a control neurone by using this protocol. τ_{deact} (time constant of deactivation) was measured by fitting single-exponential curves to the tail currents. Holding potential = −80 mV.

−80 mV), the data on deactivation must be viewed with caution because such large, rapid currents are subject to significant voltage and time course errors imposed by the series resistance.

Effects of axotomy on I_C

The Ca^{2+}-dependent K^+ current, I_C, plays a major role in the repolarization of the AP in bullfrog sympathetic ganglion B-cells (Lancaster & Pennefather, 1987). Since Ca^{2+} current is decreased, a decrease in I_C would be expected after axotomy. I_C was

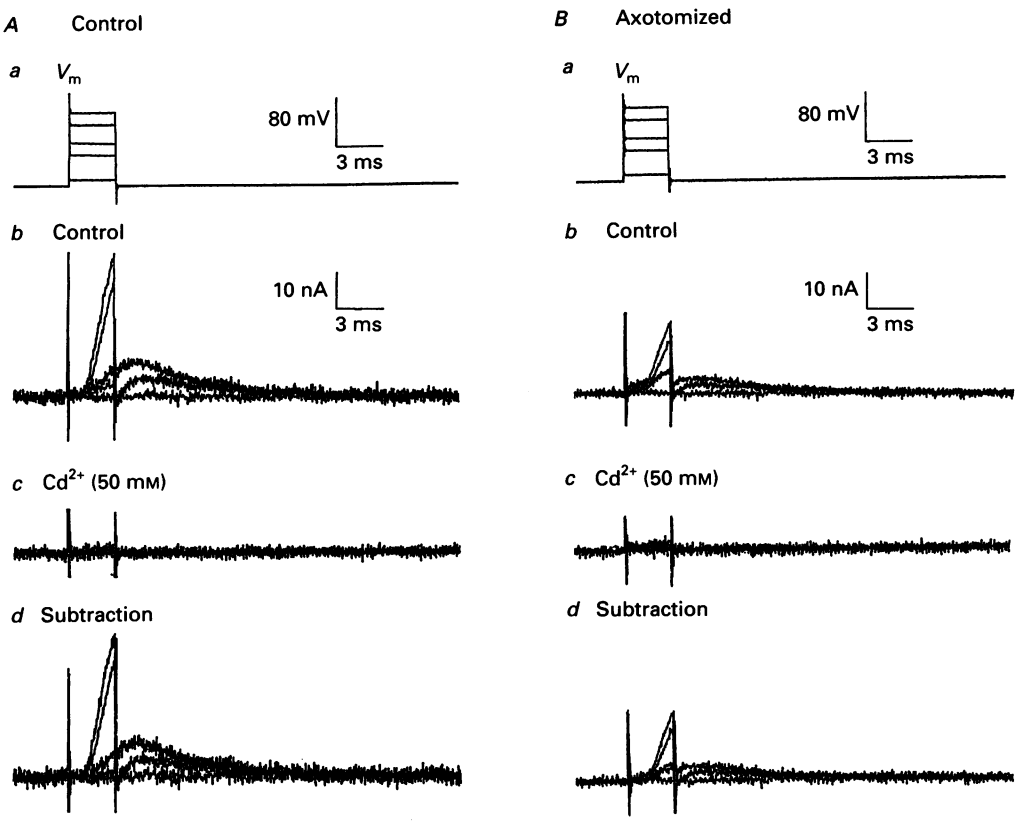

Fig. 9. Comparison of I_C in a typical control (*A*) and a typical axotomized (*B*) neurone. *a*, voltage protocol for evoking I_C. Cells were held at -40 mV and stepped to depolarized potentials for 3 ms. V_m shows the membrane voltage which the cell membrane attained in response to a step command pulse to depolarized potentials. *b*, a family of currents evoked in response to a series of depolarizing command pulses ($[Ca^{2+}]_o = 4$ mM). *c*, a family of currents evoked by same depolarizing commands as used in *c* but in the presence of 50 μM Cd^{2+}, 4 mM Mg^{2+} and $[Ca^{2+}]_o = 0$ mM to block I_{Ca} and calcium-dependent K^+ currents. *d*, I_C, in relatively pure form, obtained by subtracting current in 0 mM Ca^{2+}, 4 mM Mg^{2+} and 50 μM Cd^{2+} from that obtained in 4 mM Ca^{2+}.

evoked by applying brief (3 ms) depolarizing commands from a holding potential of -40 mV. The extracellular solution contained 4 mM Ca^{2+} but no Na^+ (see Methods). This protocol should minimize contamination of the current by the delayed rectifier (I_K) which should be largely inactivated at this potential (Adams *et al.* 1982). The decrease in I_C after axotomy is apparent from the typical current records illustrated

in Fig. 9. I_C appears as a rapidly activating outward current and the rate of activation increases with increasing depolarization. The current is almost completely eliminated by replacement of Ca^{2+} with Mg^{2+} and addition of 50 μM Cd^{2+} to the external solution. For analysis of I_C, the very small currents remaining in Cd^{2+} were

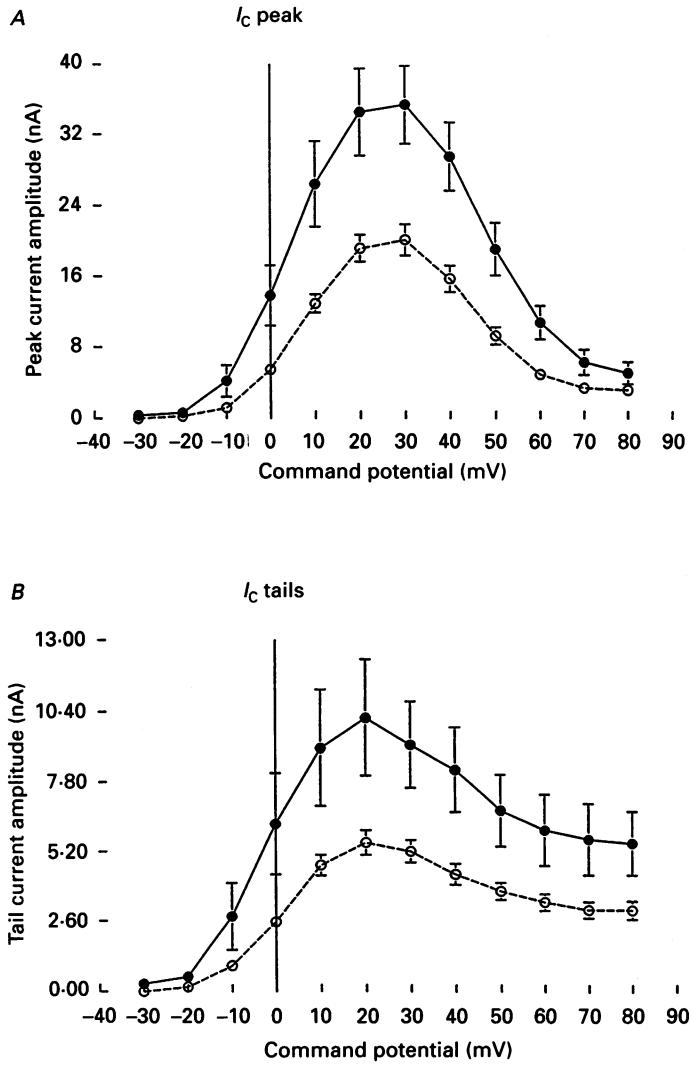

Fig. 10. Effects of axotomy on I_C. *A*, *I–V* relationship for peak current amplitudes in control (●; $n = 26$) and axotomized (○; $n = 49$) neurones. Peak current was measured at the end of a 3 ms depolarizing pulse command. *B*, *I–V* relationship for peak tail current amplitudes in control (●; $n = 26$) and axotomized (○; $n = 49$) neurones. Tail currents were measured at maximum amplitude after the end of the depolarizing command. Holding potential = −40 mV.

subtracted from the original currents. Data obtained from peak currents at the end of a 3 ms pulse to various depolarized potentials and the tail currents measured at peak amplitude following this pulse have been replotted as current–voltage

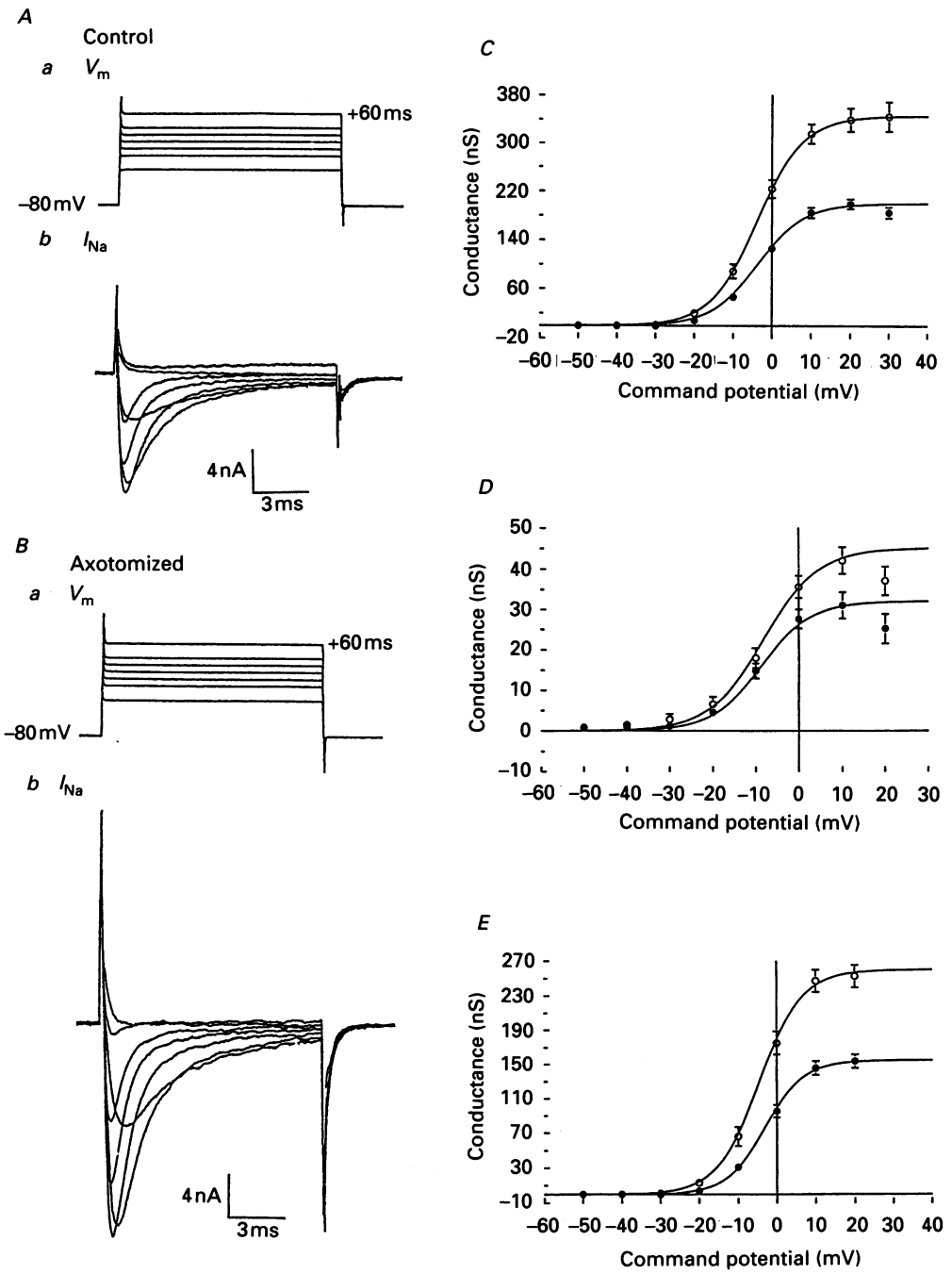

Fig. 11. Effects of axotomy on I_{Na}. Cells were held at -80 mV and step-commanded to different depolarized potentials for 12 ms and peak currents measured after filtering digitally at 4 kHz. *A* and *B* are typical recordings from a control and an axotomized neurone respectively. Panel *a* shows the membrane potential (V_m) which the cell

relationships in Fig. 10*A* and *B* respectively. The maximum amount of I_C is activated by depolarization to +20 or +30 mV. Peak and tail current values for a 3 ms step to +20 mV were 19·2±1·5 and 5·5±0·5 nA for axotomized cells ($n = 49$) and 34·5±4·9 and 10·2±2·1 nA for control cells ($n = 26$) respectively. There was therefore a significant decrease in peak and tail current amplitude after axotomy ($P < 0.005$ for peak currents and $P < 0.005$ for tails). Since the 3 ms pulse used in these experiments is too short for I_C to approach its maximum, it is possible that the reduction in current amplitude seen in axotomized neurones results from slowed activation kinetics. However, experiments using longer (50 ms) voltage commands have shown that axotomy reduces steady-state I_C and that the rate of activation is unchanged (B. S. Jassar, P. S. Pennefather & P. A. Smith, submitted).

Effects of axotomy on I_{Na}

Axotomy produced a marked potentiation of total I_{Na}. This effect is illustrated in the typical data records shown in Fig. 11. The data from the current–voltage relationship for total peak I_{Na} in thirty-seven control and thirty-seven axotomized cells were converted into conductance data. The resulting activation curves are plotted in Fig. 11*C*. Since part of the G_{Na} of bullfrog sympathetic ganglion B-cells is TTX resistant (Jones, 1987), I_{Na} was studied in the presence of 1 μM TTX in thirty-four of the thirty-seven control cell and thirty-four of the thirty-seven axotomized cells. One micromolar TTX blocked 75–80% of the total I_{Na} at −10 to +30 mV in both control and axotomized cells. The conductance–voltage relationship for the peak, TTX-resistant I_{Na} is shown in Fig. 11*D*. The TTX-resistant current appears to be slightly less affected by axotomy than the total I_{Na}. For example at +10 mV, TTX-resistant G_{Na} is increased by about 35% from 31·0±3·2 to 42·0±3·2 nS (Fig. 11*D*) whereas the total G_{Na} at the same voltage is increased by 71% (from 184·9±8·4 to 315·2±16·4 nS; Fig. 11*C*).

To illustrate more clearly the effect of axotomy on the TTX-sensitive component

---

membrane attained in response to a series of voltage-command pulses and panel *b* shows a family of I_{Na}s elicited in response to depolarizing commands. I_{Na} was converted to G_{Na} using the equation

$$G_{Na(V)} = I_{Na(V)}/(V - E_{Na}),$$

where $G_{Na(V)}$ and $I_{Na(V)}$ are peak Na^+ conductance and current at the command potential, V, and E_{Na} (for $[Na^+]_o$ = 97·5 mM and $[Na^+]_i$ = 9 mM) = +60 mV. Symbols represent the observed data points and the continuous lines are plots of the Boltzmann equation (described in legend to Fig. 2) in Fig. 11*C*, *D* and *E*. *C*, conductance–voltage relationship calculated from total peak I_{Na} in control (●; $n = 37$) and axotomized (○; $n = 37$) neurones elicited in response to commands to various depolarized potentials. V_o = −3·7 mV and slope factor = 6 mV per *e*-fold change in potential for both control and axotomized cells. *D*, conductance–voltage relationship estimated from TTX-resistant I_{Na} measured in the presence of 1 μM TTX in control (●; $n = 34$) and axotomized (○; $n = 34$) neurones. V_o = −8·7 and −8·2 mV, and slope factor = 5·75 and 6·3 mV per *e*-fold change in potential for control and axotomized neurones respectively. *E*, conductance–voltage relationship calculated from TTX-sensitive I_{Na} in control (●; $n = 34$) and axotomized (○; $n = 34$) neurones. TTX-sensitive current was obtained by subtracting TTX-resistant component from total I_{Na}. V_o = −3 and −4·5 mV, and slope factor = 5 and 5·5 mV per *e*-fold change in potential for control and axotomized neurones respectively.

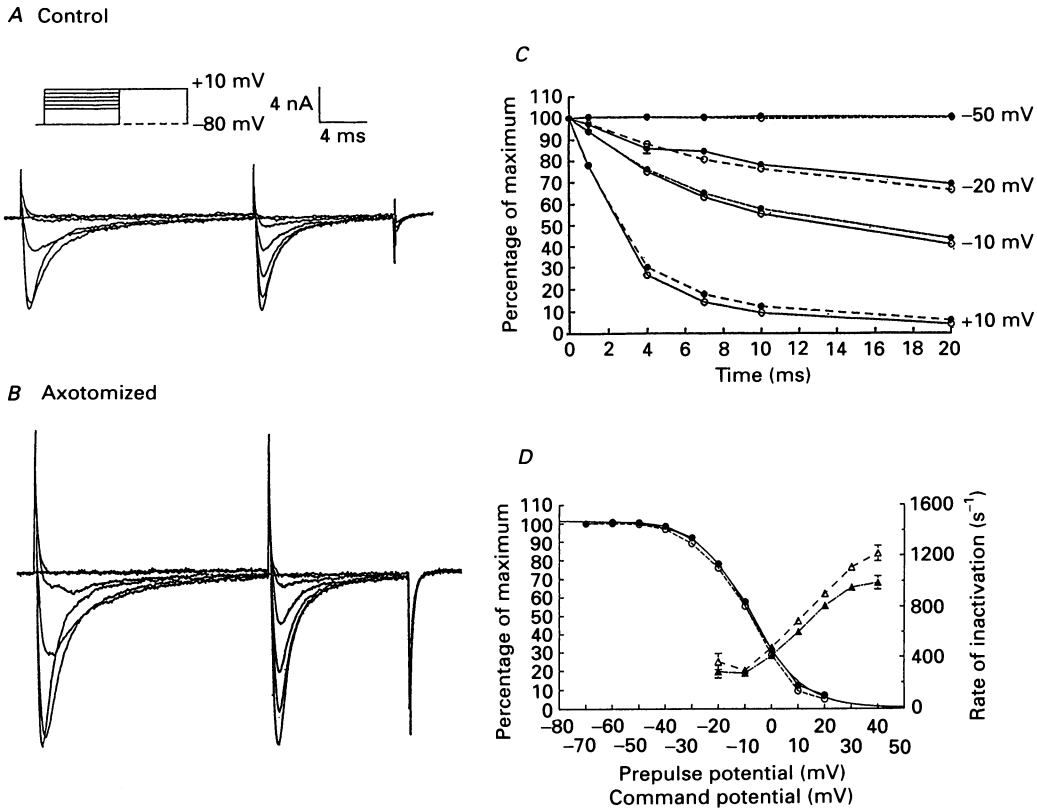

Fig. 12. Effects of axotomy on voltage and time dependence of development of inactivation of I_{Na}. *A*, upper panel (left) is the voltage protocol. The first part of the protocol is the conditioning pulse during which times cells were held at relatively depolarized potentials for 1, 4, 7, 10 or 20 ms. The amount of inactivation developed by this conditioning pulse was then tested by applying a 12 ms test pulse to +10 mV. Lower panel shows raw data records of I_{Na} evoked from a typical control cell using a series of 20 ms conditioning pulses to −40, −30, −20, −10, 0 and +10 mV followed by a test pulse to +10 mV. The first and largest current record was recorded by a test pulse to +10 mV from the holding potential of −80 mV. *B*, a family of I_{Na}s evoked from a typical axotomized neurone by using the same series of voltage protocols as for the control cell in *A*. *C*, comparison of voltage and time dependence of I_{Na} inactivation in control (●; $n = 37$) and axotomized (○; $n = 37$) neurones. Current elicited in each test pulse was converted to percentage of the maximum current elicited from the holding potential of −80 mV. *D*, plot for I_{Na} inactivation at 10 ms obtained from such data such as those in *C* for 10 ms prepulses to different potentials. The continuous line indicates a plot of the Boltzmann equation as indicated in the text. ● represents control data and ○ represents data from axotomized cells in all graphs. Relationship between rate of inactivation of I_{Na} and command potential in control (▲; $n = 37$) and axotomized (△; $n = 37$) neurones (y-axis on the right side). Rate of inactivation was calculated from τ_{inact} measured by single-exponential fits to the decay of current during 12 ms depolarizing pulses (similar to those shown in Fig. 11*C*). Note that the rate of inactivation of I_{Na} was slightly enhanced in axotomized neurones.

of I_{Na}, current–voltage plots and activation curves were replotted using data from thirty-four control and thirty-four axotomized cells following subtraction of the TTX-resistant current from the total I_{Na} in each cell. These data are presented in Fig. 11*E*. The averaged control and axotomized data in Fig. 11*C*, *D* and *E* are well

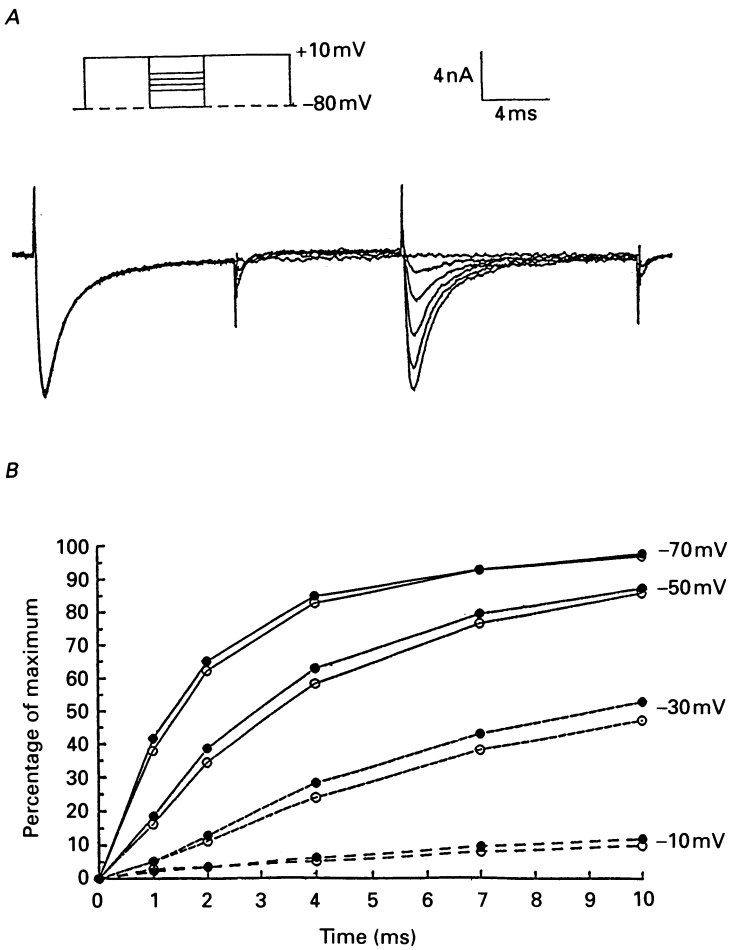

Fig. 13. Effects of axotomy on voltage and time dependence of recovery from inactivation of I_{Na}. *A*, upper panel (left) is the voltage protocol. The first part of the protocol is the conditioning pulse for inactivating I_{Na} during which the cells were stepped from the holding potential of −80 mV to +10 mV for 12 ms. The second part of the protocol is for studying time course and voltage dependence of the recovery from this inactivation. During this time, the cell was held at a series of different depolarized potentials for 1, 2, 4, 7 or 10 ms. The amount of recovery from inactivation remaining after this second part of the protocol was then tested by applying a test pulse to +10 mV. Lower panel shows raw data records of I_{Na} evoked from a typical control cell. In this part of the experiment, the test pulse to +10 mV assessed the amount of inactivation persisting after 10 ms at various potentials. *B*, comparison of voltage and time dependence of recovery of I_{Na} inactivation in control (●; $n = 37$) and axotomized (○; $n = 37$) neurones. Current elicited in each test pulse was converted to percentage of the maximum current elicited at +10 mV from the initial −80 mV holding potential.

described by a Boltzmann equation and there is no obvious shift in the voltage dependence of G_{Na} following axotomy.

The development of inactivation of I_{Na} is a time- and voltage-dependent process (Hodgkin & Huxley, 1952; Jones, 1987). The rate of onset of activation at different potentials was studied using protocols such as that illustrated in Fig. 12. The cell was clamped to a series of relatively positive holding potentials (from -50 to $+10$ mV) for 1, 4, 7, 10 and 20 ms to allow inactivation to develop prior to the application of a 12 ms test pulse to $+10$ mV. The amplitude of I_{Na} generated during this test pulse provided a measurement of the amount of inactivation which developed at various holding potentials. These data are plotted in Fig. 11*C* as the ratio of the peak current flowing in the test pulse to the maximal current which was evoked from a holding potential of -80 mV. There is no apparent difference between the data from thirty-four control and thirty-four axotomized cells. Axotomy failed to affect the voltage dependence of inactivation which was studied using a 10 ms prepulse prior to a test pulse to $+10$ mV. These data are expressed as an inactivation plot in Fig. 12*D*. The continuous line is a Boltzmann plot for fast inactivation assuming $z = 2{\cdot}6$ and $V_0 = -8$ mV.

In order to examine the possible role of changes in I_{Na} inactivation in axotomy-induced spike broadening, the inactivation time constants (τ_{inact}) were measured from data such as those shown in Fig. 11. The relationship between rate of inactivation and voltage for thirty-seven control and thirty-seven axotomized cells is plotted in Fig. 12*D*. The current appeared to inactivate slightly more rapidly in axotomized cells but this effect may have been secondary to increased clamp error associated with the larger currents in axotomized neurones.

I_{Na} recovers from inactivation very quickly and recovery is almost complete in less than 10 ms. The rate of recovery from inactivation was studied using the protocol shown in Fig. 13. The cell was held at -80 mV and stepped to $+10$ mV for 12 ms to allow I_{Na} to activate and inactivate. The cell was then held at a variety of potentials for 1, 2, 4, 7 and 10 ms to allow for recovery from inactivation. The amount of inactivation remaining at various potentials and at various time intervals was assessed by applying a test pulse command to $+10$ mV. The data from thirty-seven control and thirty-seven axotomized cells are shown in Fig. 13*B*. Inactivation is expressed as the ratio of the current in the test pulse to the amplitude of the maximal I_{Na} in the conditioning pulse. Apart from some small difference at -30 mV, the rate of recovery from inactivation was little altered by axotomy.

DISCUSSION

Mechanism of axotomy-induced spike broadening

These experiments show that the increase in spike width seen after axotomy of bullfrog sympathetic ganglion cells involves a reduction in I_{Ca} and concomitant reduction of I_C rather than from a slowing in the rate of I_{Na} inactivation. This is because the rate of I_{Na} inactivation, if anything, is increased after axotomy predicting a reduction, rather than an increase, in the duration of the AP.

In a previous study from this laboratory (Kelly *et al.* 1986) it was found that regenerative Ca^{2+} spikes could be elicited both in control and in axotomized

neurones. The interpretation of that study was that axotomy does not affect Ca^{2+} channels and that the increase in spike width and reduction in AHP amplitude and duration resulted from functional loss of Ca^{2+}-activated K^+ channels. However, the present study shows that I_{Ca} is significantly reduced in axotomized neurones. The difference between these results and those of Kelly *et al.* (1986) presumably reflects the inherent non-linearities associated with using regenerative Ca^{2+} spikes as indices of Ca^{2+} channel function.

Changes in I_{Ba} and Ca^{2+} channels

Both N- and L-type Ca^{2+} channels are present in bullfrog sympathetic neurones (Lipscombe *et al.* 1988). Based on the sensitivity of whole-cell I_{Ba} to ω-conotoxin (100 nM), BayK8644 (1 μM) and nifedipine (10 μM), Jones & Marks (1989*a*) and Jones & Jacobs (1990) suggested that N-type Ca^{2+} channels carry approximately 90% of the Ca^{2+} current in bullfrog sympathetic neurones.

Although the total I_{Ba} was reduced after axotomy, there are no obvious differences in the shape of the *I–V* relationship. Interestingly, ω-conotoxin reduces the total current to about the same absolute level in both control and axotomized cells. This suggests that the effects of axotomy are restricted to changes in N-type Ca^{2+} channels. This idea is supported by the observation that BayK8644 was able to induce a similar amount of L-type Ca^{2+} current in control and axotomized neurones and this additional current was subject to a similar amount of reduction by nifedipine in both situations.

It has often been suggested that axotomy causes differentiated neurones to revert to an 'immature' state (Lieberman, 1971; Gurtu & Smith, 1988). it has been reported that during development of several neuronal types, 'low-voltage-activated' (T-type) Ca^{2+} channels are expressed either before 'high-voltage-activated' Ca^{2+} channels or transiently (Gottmann, Dietzel, Lux, Huck & Rohrer, 1988; Pirchio, Lightowler & Crunelli, 1990; Thompson & Wong, 1991). There was no indication of the presence of a T-type Ca^{2+} conductance either from the shape of the *I–V* curve between -60 and -20 mV (Fig. 5*B* and *D*) as is seen in sensory neurones (see Fig. 1*D* and *E* in Fox, Nowycky & Tsien, 1987; and Fig. 4*B* in Gottmann *et al.* 1988) or from the I_{Ba} traces shown in Fig. 1*B*.

The small changes in the rate of I_{Ba} activation and deactivation observed after axotomy must be interpreted with caution, because the currents seen after axotomy are smaller and thus less susceptible to distortion as a result of series resistance. The lack of effect of axotomy on the voltage dependence of I_{Ba} activation (Fig. 2*E*) and the doubtful significance of the small changes in kinetics (Fig. 8) suggest that at least in terms of their activation parameters, the Ca^{2+} channels present in axotomized cells are similar to those in control cells. The simplest interpretation for the decrease in I_{Ba} is that fewer activatable channels are present in the neuronal cell body after axotomy at normal membrane potentials.

By contrast with the slight effects of axotomy on I_{Ba} activation, inactivation is clearly enhanced in axotomized neurones. We have observed at least three components of inactivation in both control and axotomized neurones: 'fast', 'intermediate' and 'slow'. 'Fast' and 'intermediate' components of inactivation are almost doubled after axotomy (Table 1) and the voltage where slow inactivation is half maximal is shifted at least 10 mV more negative after axotomy.

Although some effects on the time course of 'fast' and 'intermediate' components were observed, these effects were less well defined. Most of the changes in I_{Ba} associated with axotomy may be due to changes in the activation properties of Ca^{2+} channels. Thus axotomy may cause more of the Ca^{2+} channels to switch from a 'non-inactivating' to an 'inactivating mode' after axotomy (Plummer & Hess, 1991). Although the factors that influence the equilibrium between these modes are not completely understood, phosphorylation has recently been shown to increase the proportion of inactivating Ca^{2+} channels in bullfrog sympathetic ganglion neurones (Wertz *et al.* 1993). It is therefore possible that the changes in inactivation seen after axotomy result from alterations in Ca^{2+} channel phosphorylation.

Another possibility is that axotomy produces a change in subunit structure or stoichiometry of different subunits in the channel macromolecule as a result of changes at the transcriptional or post-transcriptional level. Precedence for this idea comes from the observation that heterologous expression of different subunits of L-type Ca^{2+} channels from skeletal muscle in LCa.11 cells induces Ca^{2+} channels which exhibit I_{Ca} with different kinetic properties. Expression of the α-subunit alone results in the induction of I_{Ca} with slow activation and inactivation kinetics whereas co-expression of α and β subunits induces channels which have faster kinetics (Varadi, Lory, Schultz, Varadi & Schwartz, 1991). This suggests that different functions of the channel are vested in different subunits. A third possibility is that increased I_{Ba} inactivation results from axotomy-induced cytoskeletal disruption (Fukuda, Kameyama & Yamaguchi, 1981; Johnson & Byerly, 1993).

Changes in I_{Na}

The increase in amplitude of I_{Na} may be responsible for the small, yet significant increase in spike height seen in axotomized bullfrog sympathetic ganglion neurones (Gordon *et al.* 1987). Indeed, this effect may be a general characteristic of axotomized cells because the rate of rise of the AP is known to increase in a wide variety of vertebrate and invertebrate neuronal types after axotomy (Gallego *et al.* 1987; Titmus & Faber, 1990). As with the Ca^{2+} channels, the molecular mechanism underlying the increased G_{Na} could result from changes in channel subunit expression, post-translational modification or changes in channel distribution.

Effects of axotomy on ion channels

During development, several types of nerve cells express TTX-resistant Na^+ channels. Also, some types of immature cells exhibit Ca^{2+}-dependent rather than Na^+-dependent APs (Spitzer, 1979; Nerbonne & Gurney, 1989, but see also Barish, 1986) whilst others may transiently express T-type Ca^{2+} currents (Gottmann *et al.* 1988; Pirchio *et al.* 1990; Thompson & Wong, 1991). One working hypothesis which seeks to explain the 'cell body reaction' is that it reflects dedifferentiation of neurones towards an immature state which is more amenable to growth processes (Lieberman, 1971; Titmus & Faber, 1990). This dedifferentiation concept does not fit with the observed effects of axotomy on ion channels in bullfrog sympathetic ganglia. This is because axotomy did not potentiate TTX-resistant I_{Na} any more than TTX-sensitive I_{Na}. Furthermore, I_{Ba} was decreased rather than increased and no T-type Ca^{2+} current was seen after axotomy.

An increase in the rate of rise and amplitude of the AP is a fairly consistent observation following axotomy of a variety of neuronal types (Gallego *et al.* 1987) whereas changes in AHP amplitude and duration and spike width are more variable (Titmus & Faber, 1990). It is possible, however, that N-type Ca^{2+} channels are always affected and tend to assume an 'inactivating' mode after axotomy. The differential effects of axotomy on the AP in various neuronal types would then reflect the expression and level of inactivation of N-type Ca^{2+} channels in each type of neurone. It will obviously be necessary to examine a wide variety of neuronal types before one can advance a general hypothesis relating changes in ion channels to the axotomy-induced cell body reaction.

APPENDIX

The kinetics of the slow component of I_{Ba} inactivation were deduced from the use-dependent build-up of 'slow' inactivation during a train of commands to 0 mV from a holding potential of −80 mV where few channels are open and few channels are in the 'slow' inactivated state at equilibrium. At a potential (0 mV) where all of the channels can open and 'slow' inactivation can be complete, the proportion (O_n) of Ca^{2+} channels activated by the nth pulse in a train will be equal to the proportion (R_{n-1}) of channels that are in a non-inactivated, resting state at −80 mV just before that pulse (i.e. $R_{n-1} = O_n$). If k_+ is the rate constant of inactivation at 0 mV, inactivation during the command will proceed at a rate initially equal to $O_n k_+$ and decrease to $O_{n+1} k_+$ at the end of the pulse. This assumes that all states of the channel enter the 'slow' inactivation state at the same rate. Provided the fraction of the peak current that undergoes 'slow' inactivation during the pulse is not large (e.g. $O_{n+1} \simeq O_n$), the amount of inactivation that develops during a pulse of duration t_1 will be $O_n k_+ t_1$ which can also be written as $R_{n-1} k_+ t_1$. Similarly, if k_- is the rate constant for recovery from inactivation at −80 mV and the interval between pulses, t_2, is such that there is little recovery before the next pulse is initiated, the proportion of inactivated channels that does recover will equal $(1-R_n) k_- t_2$.

$$\therefore R_{n-1} - R_n = R_{n-1} k_+ t_1 - (1-R_n) k_- t_2. \tag{A1}$$

Eventually the total decrement will approach a limiting value $(1-R_\infty)$ where $R_{n-1} - R_n = 0$. Thus, from eqn (A1)

$$R_\infty k_+ t_1 = (1-R_\infty) k_- t_2, \tag{A2a}$$

and

$$R_\infty = \frac{k_- t_2}{k_+ t_1 + k_- t_2}. \tag{A2b}$$

The decrement per pulse appears to decline exponentially. This means that

$$\ln\left(\frac{R_n - R_\infty}{R_{n-1} - R_\infty}\right) = -\lambda,$$

where λ is a constant. For small values of λ

$$\ln(1-\lambda) \simeq -\lambda.$$

Therefore

$$\frac{R_n - R_\infty}{R_{n-1} - R_\infty} = 1 - \lambda,$$

and

$$\lambda = \frac{R_{n-1} - R_n}{R_{n-1} - R_\infty}.$$

Substituting eqn (1) and (2*b*) one obtains

$$\lambda = \frac{R_{n-1} k_+ t_1 - (1 - R_n) k_- t_2}{R_{n-1} - [k_- t_2 / (k_- t_2 + k_+ t_1)]},$$

$$= (k_- t_2 + k_+ t_1) \left[\frac{R_{n-1} k_+ t_1 - (1 - R_n) k_- t_2}{R_{n-1} k_+ t_1 - (1 - R_{n-1}) k_- t_2} \right].$$

Again, if λ is small then $R_{n-1} \simeq R_n$ and,

$$\lambda \simeq k_- t_2 + k_+ t_1. \tag{A3}$$

Supported by a Medical Research Council (MRC) of Canada grant to P.A.S. The Alberta Heritage Foundation for Medical Research provided some items of major equipment, travel grants and a studentship to B.S.J.; B.S.J. is also an MRC fellow and P.A.S. was an Alberta Heritage Medical Scholar, P.S.P. is a Career Scientist of the Ontario Ministry of Health. We thank Dr Stephen W. Jones for his comments on an early version of this manuscript.

REFERENCES

ADAMS, P. R., BROWN, D. A. & CONSTANTI, A. (1982). M-currents and other potassium currents in bullfrog sympathetic neurones. *Journal of Physiology* **330**, 537–572.

BARISH, M. E. (1986). Differentiation of voltage-gated potassium current and modulation of excitability in cultured amphibian spinal neurones. *Journal of Physiology* **375**, 229–250.

BELMONTE, C., GALLEGO, R. & MORALES, A. (1988). Membrane properties of primary sensory neurones of the cat after peripheral reinnervation. *Journal of Physiology* **405**, 219–232.

CARLSEN, R. C., KIFF, J. & RYUGO, K. (1982). Suppression of the cell body response in axotomized frog spinal neurones does not prevent initiation of nerve regeneration. *Brain Research* **234**, 11–25.

CZEH, G., KUDO, N. & KUNO, M. (1977). Membrane properties and conduction velocity in sensory neurones following central and peripheral axotomy. *Journal of Physiology* **270**, 165–180.

DODD, J. & HORN, J. P. (1983). A reclassification of B- and C-cells in the ninth and tenth paravertebral sympathetic ganglion of the bullfrog. *Journal of Physiology* **334**, 255–269.

ELMSLIE, K. S., KAMMERMEIER, P. J. & JONES, S. W. (1992). Calcium current modulation in frog sympathetic neurones: L-current is relatively insensitive to neurotransmitters. *Journal of Physiology* **456**, 107–123.

FINKEL, A. S. & REDMAN, S. J. (1984). Theory and operation of a single microelectrode voltage clamp. *Journal of Neuroscience Methods* **11**, 101–127.

FOX, A. P. NOWYCKY, M. C. & TSIEN, R. W. (1987). Kinetic and pharmacological properties distinguishing three types of calcium current in chick sensory neurones. *Journal of Physiology* **394**, 149–172.

FUKUDA, J., KAMEYAMA, M. & YAMAGUCHI, K. (1981). Breakdown of cytoskeletal filaments selectively reduces Na and Ca spikes in cultures mammal neurones. *Nature* **294**, 82–85.

GALLEGO, R., IVORRA, I. & MORALES, A. (1987). Effects of central or peripheral axotomy on membrane properties of sensory neurones in the petrosal ganglion of the cat. *Journal of Physiology* **391**, 39–56.

GOH, J. W., KELLY, M. E. M. & PENNEFATHER, P. S. (1989). Electrophysiological function of the delayed rectifier (I_K) in bullfrog sympathetic ganglion neurones. *Pflügers Archiv* **413**, 482–486.

GORDON, T., KELLY, M. E. M., SANDERS, E. J., SHAPIRO, J. & SMITH, P.A. (1987). The effect of axotomy on bullfrog sympathetic neurones. *Journal of Physiology* **392**, 213–229.

GOTTMAN, K., DIETZEL, I. D., LUX, H. D., HUCK, S. & ROHRER, H. (1988). Development of inward currents in chick sensory and autonomic neuronal precursor cells in culture. *Journal of Neuroscience* **8**, 3722–3732.

GRAFSTEIN, B. & MCQUARRIE, E. I. (1978). Role of nerve cell body in axonal regeneration. In *Neuronal Plasticity*, pp. 155–195, ed. COTMAN, C. W., Raven Press, New York.

GURTU, S. & SMITH, P. A. (1988). Electrophysiological characteristics of hamster DRG cells and their response to axotomy. *Journal of Neurophysiology* **59**, 408–423.

GUSTAFSSON, B. & PINTER, M. K. (1984). Effects of axotomy on distribution of passive electrical properties of cat motoneurones. *Journal of Physiology* **356**, 433–442.

HODGKIN, A. L. & HUXLEY, A. F. (1952). A quantitative description of membrane current and its application to conduction and excitation in nerve. *Journal of Physiology* **117**, 500–544.

JASSAR, B. S. & SMITH, P. A. (1991*a*). Role of target organ in the maintenance of calcium currents in bullfrog sympathetic neurones. *Society for Neuroscience Abstracts* **17**, 67.

JASSAR, B. S. & SMITH, P. A. (1991*b*). Slow frequency-dependence of action potential after hyperpolarization in bullfrog sympathetic ganglion neurones. *Pflügers Archiv* **19**, 478–485.

JASSAR, B. S. & SMITH, P. A. (1992). Mechanism of axotomy-induced spike broadening in bullfrog sympathetic neurones. *Society for Neuroscience Abstracts* **18**, 42.

JOHNSON, B. D. & BYERLY, L. (1993). A cytoskeletal mechanism for calcium channel rundown and block by intracellular calcium. *Biophysical Journal* **64**, A116.

JONES, S. W. (1987). Sodium currents in dissociated bull-frog sympathetic neurones. *Journal of Physiology* **389**, 605–627.

JONES, S. W. & JACOBS, L. S. (1990). Dihydropyridine actions on calcium currents of frog sympathetic neurones. *Journal of Neuroscience* **10**, 2261–2267.

JONES, S. W. & MARKS, T. N. (1989*a*). Calcium currents in bullfrog sympathetic neurones; I. Activation, kinetics and pharmacology. *Journal of General Physiology* **94**, 151–167.

JONES, S. W. & MARKS, T. N. (1989*b*). Calcium currents in bullfrog sympathetic neurones; II. Inactivation. *Journal of General Physiology* **94**, 169–182.

KELLY, M. E. M., GORDON, T., SHAPIRO, J. & SMITH, P. A. (1986). Axotomy affects calcium-sensitive potassium conductance in sympathetic neurones. *Neuroscience Letters* **67**, 163–168.

LAIWAND, R., WERMAN, R. & YAROM, Y. (1988). Electrophysiology of degenerating vagal motor nucleus of the guinea-pig following axotomy. *Journal of Physiology* **404**, 749–766.

LANCASTER, B. & PENNEFATHER, P. (1987). Potassium currents evoked by brief depolarizations in bull-frog sympathetic ganglion cells. *Journal of Physiology* **387**, 519–548.

LIEBERMAN, A. R. (1971). The axon reaction: A review of the principal features of perikaryal responses to axon injury. *International Review of Neurobiology* **14**, 49–124.

LIPSCOMBE, D., MADISON, D. V., POENIE, M., REUTER, H., TSIEN, R. Y. & TSIEN, R. W. (1988). Spatial distribution of calcium channels and cytosolic calcium transients in growth cones and cell bodies of sympathetic neurones. *Proceedings of the National Academy of Sciences of the USA* **85**, 2398–2402.

MORRILL, J., BOLAND, L. M. & BEAN, B. P. (1991). ω-Conotoxin block of calcium channels in peripheral neurons: Reversibility and the influence of divalent cation concentration. *Society for Neuroscience Abstracts* **17**, 1160.

NERBONNE, J. N. & GURNEY, A. M. (1989). Development of excitable membrane properties in mammalian sympathetic neurons. *Journal of Neuroscience* **9**, 3272–3280.

PIRCHIO, M., LIGHTOWLER, S. & CRUNELLI, V. (1990). Postnatal development of the T calcium current in cat thalamocortical cells. *Neuroscience* **38**, 39–45.

PLUMMER, M. R. & HESS, P. (1991). Reversible uncoupling of inactivation in N-type calcium channels. *Nature* **351**, 657–659.

SALA, F. (1991). Activation kinetics of calcium currents in bull-frog sympathetic neurones. *Journal of Physiology* **437**, 221–238.

SPITZER, N. C. (1979). Ion channels in development. *Annual Review of Neuroscience* **2**, 263–297.

THOMPSON, S. M. & WONG, R. K. S. (1991). Development of calcium current subtypes in isolated rat hippocampal pyramidal cells. *Journal of Physiology* **439**, 671–689.

TITMUS, M. J. & FABER, D. S. (1990). Axotomy-induced alterations in the electrophysiological characteristics of neurones. *Progress in Neurobiology* **35**, 1–51.

VARADI, G., LORY, P., SCHULTZ, D., VARADI, M. & SCHWARTZ, A. (1991). Acceleration of activation and inactivation by β subunit of the skeletal muscle calcium channel. *Nature* **352**, 159–162.

WERTZ, M. A., ELMSLIE, K. S. & JONES, S. W. (1993). Phosphorylation enhances inactivation of N-type calcium channel current in bullfrog sympathetic ganglion neurones. *Pflügers Archiv* (in the Press).